Hydrogeology Journal
https://doi.org/10.1007/s10040-024-02824-9

PAPER

Delineating aquitard characteristics within a Silurian dolostone aquifer using high-density hydraulic head and fracture datasets

G. Medici[1,2] · J. D. Munn[1] · B. L. Parker[1]

Received: 30 September 2023 / Accepted: 10 August 2024

Abstract

Fractured aquifers are heterogeneous due to the variable frequency, orientation, and intersections of rock discontinuities. A ~100-m-thick Silurian dolostone sequence provides a bedrock aquifer supplying the city of Guelph, Canada. Here, fracture network characteristics and associated influences on hydraulic head were examined using several data types obtained from 24 cored holes in a study that is novel for the quantity and quality of data. High (50–90°) angle joint orientations, heights, and terminations relative to bedding features were determined from acoustic televiewer logs and outcrop scanlines. These data were compared to high-resolution hydraulic head profiles showing head loss over depth-discrete intervals identifying zones with lower vertical hydraulic conductivity. This study reveals that the marl-rich Vinemount Member, traditionally considered the principal aquitard, corresponds to head loss in only 62% of the 24 boreholes. The vertical position of head loss varies across the 90-km^2 study area and occurs in any of the lithostratigraphic units of the Lockport Group. Within this sedimentary sequence, aquitards are laterally discontinuous or "patchy" at variable depths and relate to: (1) the frequency of the high-angle joints; (2) shorter joint height; and (3) the type of joint terminations. The head loss occurs in thin (2–2.5 m) intervals where the frequency of the high-angle joints is low. Where a large proportion of small joints cross-cut marl bedding planes, head loss is negligible, suggesting that the vertical hydraulic conductivity is not reduced. Overall, these findings are potentially applicable to assessing aquitard and cap rock integrity in carbonate sedimentary sequences worldwide.

Keywords Fracture network characteristics · Hydraulic head loss · Aquitard delineation · Carbonate rock aquifer · Heterogeneity · Canada

Introduction

Globally, fractured sedimentary bedrock aquifers underlie ~70% of the earth's land surface and supply ~30% of the world's population with drinking water (Berkowitz 2002; Hartmann et al. 2014). A range of contaminants from industrial and agricultural activities, including PFAS, chlorinated organic solvents, pathogens, pesticides, pharmaceuticals, nitrate, sulphate, and chloride, can reach these aquifers (Medici and West 2023; Meyer et al. 2023; Lorenzi et al. 2024). Animal waste applied directly to the land from grazing animals, or applied to land as farmyard manure or slurry, represents a key source of nitrate, viruses, and bacteria, making them widespread and common groundwater contaminants (Wakida and Lerner 2005; Rivett et al. 2008). Travel times of these contaminants from surface inputs to water supply wells can be greatly increased by the presence of overlying aquitards, which are characterized by low vertical hydraulic conductivities. Despite the heterogeneity and unpredictability in the subsurface, aquitards are typically assumed to be aligned with lithostratigraphic units, even in bedrock, at the scale of either geological members or formations in groundwater flow and contaminant transport models (e.g., Neymeyer et al. 2007; Ely et al. 2011; Medici et al. 2023a). Additionally, despite the geological nature of aquitards, a hydraulic data-driven investigation to identify the head loss and corresponding vertical component of hydraulic gradients typically observed at aquitard units is

✉ G. Medici
giacomo.medici@uniroma1.it

✉ B. L. Parker
bparker@uoguelph.ca

[1] Morwick G360 Groundwater Research Institute, College of Engineering and Physical Sciences, University of Guelph, 50 Stone Road E, Guelph, ON N1G 2W1, Canada

[2] Now at Department of Earth Sciences, Sapienza University of Rome, Piazzale Aldo Moro 5, 00185 Rome, Italy

Published online: 19 September 2024

often not combined with a characterization of stratigraphic and mechanical features to inform the position of aquitards. In other words, hydraulic properties are typically inferred from rock type rather than confirmed using detailed hydraulic head data (Meyer et al. 2008, 2016; Runkel et al. 2018).

Investigations of rock discontinuities to study fractured sedimentary aquifers are useful to inform discrete fracture network models for contaminant transport (e.g. studies of the Palaeozoic and Mesozoic sandstones of China and north-western Europe; Tellam and Barker 2006; Hitchmough et al. 2007; Xie et al. 2021), are time-intensive and uncommonly used in practice; therefore, most discontinuity studies are limited by small fracture datasets. One of the most detailed hydro-structural studies of a fractured sandstone aquifer combines acoustic televiewer (ATV) logs from vertical boreholes and scanline surveys to characterize the fracture network in the Triassic sandstones of Great Britain (Hitchmough et al. 2007), but with the absence of inclined boreholes and high-resolution hydraulic head profiles. Most similar to the research presented here, Meyer et al. (2008, 2014, 2016) and Runkel et al. (2018) defined hydraulic units in an Ordovician sequence of sandstones, siltstones, shales, and dolostones in Wisconsin USA using high-resolution hydraulic head profiles and sequence stratigraphic boundaries, but without incorporating statistics for rock discontinuities acquired either in outcrops or boreholes.

A greater amount of fracture data is available for carbonate rocks (e.g., limestone and dolostone) relative to siliciclastic rocks (Kosakowski and Berkowitz 1999; Berkowitz 2002; Odling et al. 2013; Parker et al. 2019), due in part to an assumption that fractures represent negligible flow-pathways in siliciclastic aquifers; therefore, fractures were not intensively characterized for many years in sandstones. Recent hydrogeological investigations of the Carboniferous limestones of Burren in western Ireland have produced discontinuity statistics from outcrops and treated the aquifer as a mass of undivided fractured rocks to constrain the effective (i.e. fracture) porosity (Moore and Walsh 2021). The Permian Dolostone in Great Britain and the Cretaceous Chalks in north-western Europe and Israel were recently investigated by using optical and acoustic televiewer logs to characterize the rock discontinuities (Witthüser et al. 2006; Maurice et al. 2012; Medici et al. 2019; Agbotui et al. 2020). In all these studies, the aquitard units were inferred to be systematically associated with marly, shaly, and evaporitic geological formations that represent stasis of carbonate production in the sedimentary record but were not confirmed with direct hydraulic measurements. In contrast, this study only uses litho-stratigraphy from continuous core and geophysical logs as a starting point to organize rock discontinuity statistics without defining a priori aquifer and aquitard units. Additionally, this study is the most data-intensive characterization undertaken, given the number of continuously cored boreholes with centimeter-scale logs distributed across the study area, depth resolution of hydraulic head, and number of fractures recorded using borehole geophysical ATV logs in vertical and inclined boreholes. The research is particularly distinct among investigations in fractured carbonates, due to the comparison of geophysical borehole data with a robust characterization of fractures mapped in outcrops. The novelty of this study also relates to the combination of quality and quantity of fracture data with the high ($\leq$2 m) spatial vertical resolution of hydraulic head profiles at two dozen (24) locations across the study area, associating fracture conditions in one-dimensional (1D) boreholes and two-dimensional (2D) scanlines with both geologic and hydrogeologic zones where head loss occurs. A new classification scheme to describe the joint terminations at bedding planes is also proposed to improve outcrop scanline surveys for characterization of fractured rocks.

In this paper, robust statistics are derived from carbonate rock discontinuities from the Silurian dolostone of the study area using: (1) data from outcrop scanlines along three orientations, two nearly orthogonal vertical faces and horizontal quarry pavement, (2) nine inclined and 29 vertical boreholes with vertical profiles of hydraulic head, and (3) detailed logging of lithostratigraphy obtained from continuous cores, and/or natural gamma logs. This Silurian rock sequence represents an important groundwater resource for nearly 500,000 people in both rural and urban communities including the city of Guelph and has been the focus of previous hydro-structural investigations (Lemieux et al. 2006; Parker et al. 2019; Howroyd and Novakowski 2021a, b, 2022); however, these previously published studies did not focus on the presence of aquitards and did not integrate fracture data from multiple boreholes and outcrops. Nunes et al. (2021) examined hydraulic head along with baseline hydrochemistry and isotopes from multilevel wells and well nests throughout the same study area to assess the effect of urban, industrial, and agricultural activities on groundwater flow system quality. Historically, the intermediate aquitard within the Silurian dolostone sequence was assigned to a shale-rich Vinemount Member of the Eramosa Formation. This assumption was based on lithostratigraphic information from cores and single-borehole pumping tests with screens partially penetrating the geological members of the Lockport Group (Priebe et al. 2019; Brunton and Brintnell 2020). The resolution of pumping tests penetrating multiple units is low, and the aquitard was, by default, assigned to the shale-rich Vinemount Member of the Eramosa Formation. It is common for hydrogeological investigations in the area to install two nested wells with one "shallow" above the Vinemount Member, and one "deep" in the Gasport Formation. Any head difference between the two nested wells is typically

assigned to the Vinemount Member due to its shaly nature, without having the resolution to measure the true position of head loss.

The overall aim of this paper is to inform the position and cause of aquitard occurrence in the local Silurian dolostone aquifer using an analysis of the fracture network statistics and high spatial resolution hydraulic head profiles. This dataset will be tied to the current lithostratigraphic framework to advance sedimentological and structural geologic controls on aquifer properties in a heterogeneous carbonate aquifer system. Specific research objectives of this study are: (1) present statistics of the rock discontinuities in the Silurian Lockport Group beneath the city of Guelph, (2) identify the sedimentological and structural geology factors that control significant variation in vertical hydraulic gradients/connectivity in the dolostone sequence, (3) define the styles of occurrence of the head loss, and (4) propose a new conceptual model of the dolostone aquifer-aquitard system by using multiple complementary datasets (e.g., natural gamma, ATV and high-resolution hydraulic head profiles).

Site description

Geological setting

The 95-km^2 study area encompasses the city of Guelph (population over 143,474 from Statistics Canada, 2023) located in southwestern Ontario, ~28 km east of Waterloo and 100 km west of Toronto, ON, Canada (Fig. 1a–c). The city of Guelph relies exclusively on groundwater pumped from wells and a spring collection system for its water supply.

This Silurian dolostone sequence in the Guelph area ranges from 55 to 100 m thick, and is part of the Lockport Group, containing four formations that include from oldest to youngest: Gasport, Goat Island, Eramosa and Guelph formations (Fig. 2a–c). The Gasport and Guelph Formations are dominated by dolostone beds and are related to shallow marine environments (Brunton and Brintnell 2020). The lowermost Gasport Formation is comprised of white-to-bluish-grey grainstones and packstones. This portion of Gasport Formation can also be recognized in the field by the presence of stacked crinoidal-microbial reef mounds and cross-bedding structures (Brunton and Brintnell 2020). The Guelph Formation has a light-brown colour and consists of medium-thick-to-thick dolostone beds and cross-stratified packstones (Brett et al. 1990; Brunton and Brintnell 2020). The Guelph Formation is divided into the Wellington (lower) and Hanlon (upper) members, which are dominated by reef and lagoon facies, respectively (Brunton and Brintnell 2020).

The Goat Island and Eramosa formations are dolostones with varying amounts of shale interbeds. The carbonate fraction of such interbeds ranges from 35 to 65% and is therefore described as marls for consistency with the USGS definition (Carter 2002). Of note, Huh et al. (1977) introduced the term marls in the Lockport Group in Ontario and provided a sedimentological description.

The Goat Island Formation is formally divided into the Niagara Falls (lower) and Ancaster (upper) members. The latter contains cherty nodules and a finely crystalline texture, and the lower member is a crinoidal encrinite and can be distinguished by its pin-striped appearance and slightly higher natural gamma response (Brunton and Brintnell 2020). The Eramosa Formation—Figs. 3, 4 and 5, and Fig. S1 of the electronic supplementary material (ESM)—is formally divided from the bottom to the top of the stratigraphic sequence into Vinemount, Reformatory Quarry, and Stone Road members. The Vinemount Member, whose marl beds are related to episodes of relative sea level rise (Brunton and Brintnell 2020), is a marly dolostone and contains the highest marl content within the Lockport Group. By contrast, the Reformatory Quarry Member is dominated by coarsely crystalline dolostones with coral stromatoporoid biostromal facies. The Stone Road Member is also more carbonatic than the Vinemout Member, and is characterized by finely crystalline dolostones. The Stone Road is finer grained with respect the Reformatory Quarry Member of the Eramosa Formation (Brunton and Brintnell 2020).

In southern Ontario, the deposits of the Lockport Group are layered and gently dipping (<2° degrees to the southwest as shown in Fig. 2a–c) due to lack of significant effects of orogenesis syn- and post Silurian time (Perrin et al. 2011). These carbonate deposits typically contain high-angle joints due to the far field effects of the Appalachian belt, the presence of an irregular basement, and the lithospheric glacial rebound that occurred during the Quaternary (Eyles et al. 1997; Underwood et al. 2003). Previous quarry and borehole observations of the larger-scale bedrock fracturing pattern were part of the drilling program associated with the deep geological repositories for nuclear waste storage and distinguished three principal directions of such joints: NNE–SSW, ENE–WSW and NE–SW striking in the Guelph area (Formenti et al. 2023). The dominant direction of these subvertical joints does not change significantly comparing nearby outcrops of different lithostratigraphic units in Rockwood, which is located 10 km to the east of Guelph (Kunert and Coniglio 2002; Cole et al. 2009).

Hydrogeological setting

The city of Guelph relies almost exclusively on groundwater for water supply from the underlying Silurian dolostone aquifers that are the focus of this research. These Silurian dolostones are overlain by Quaternary glacial sediments that are generally thin within the city of Guelph, typically

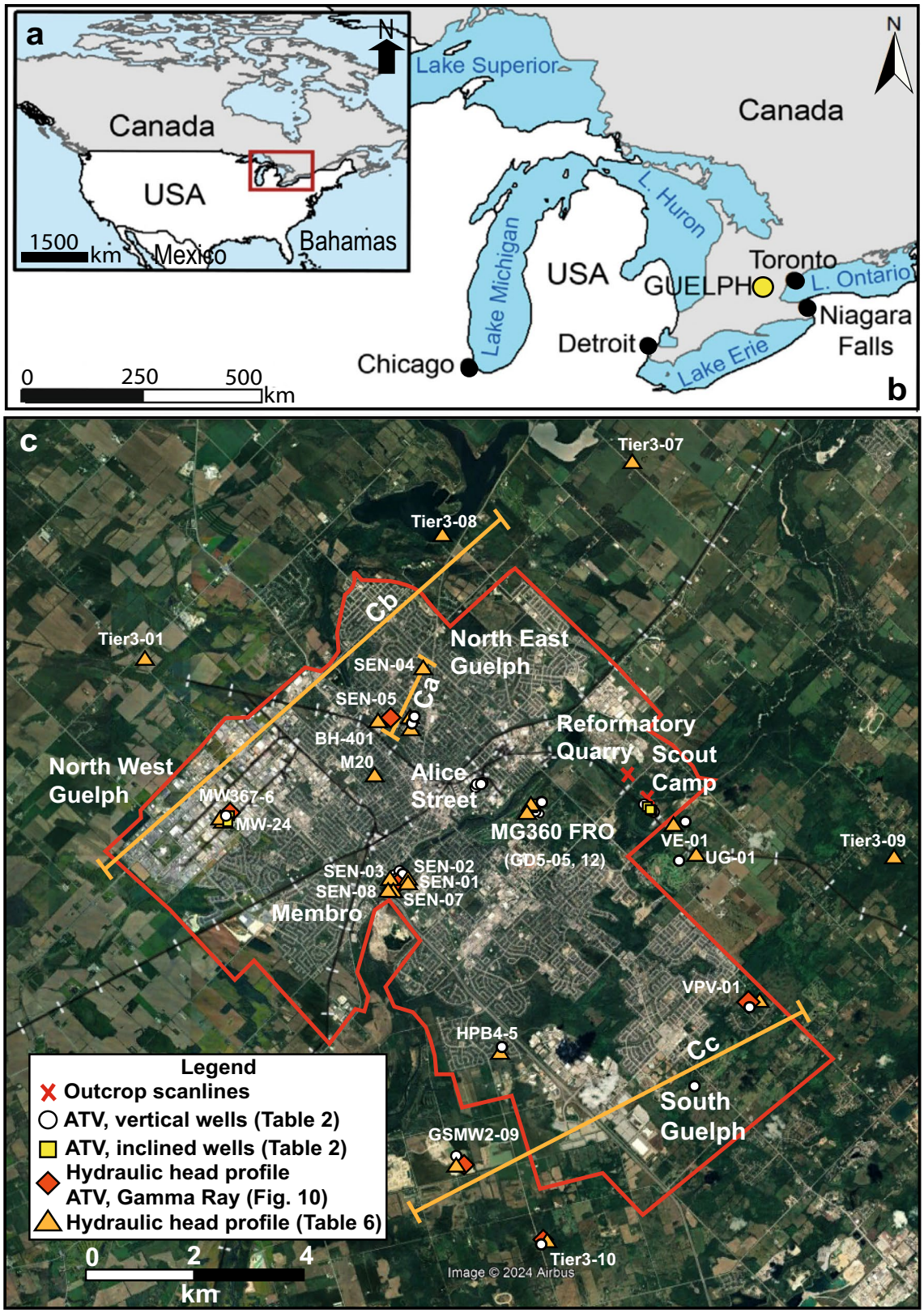

Fig. 1 Study area. **a** North America, **b** Guelph in Ontario, Canada and neighbouring areas in the United States of America, **c** City of Guelph, including the location of quarries, boreholes with ATV, gamma-ray and hydraulic head profiles and position of geological cross sections (Ca–Cc in Fig. 2)

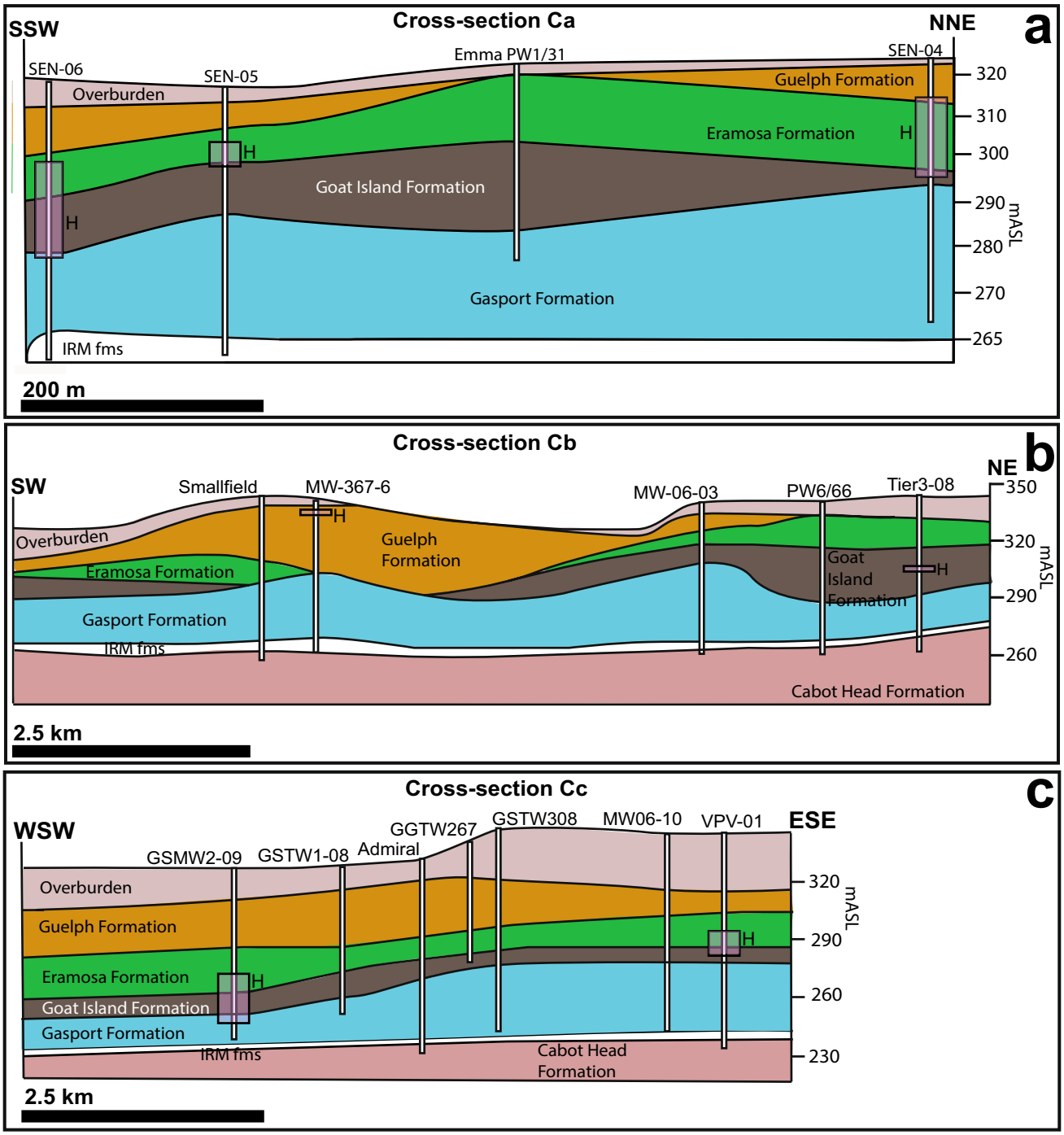

Fig. 2 Geological cross-sections (modified from Nunes et al. 2021) showing the Cabot Head Formation, Irondequoit Rockway and Merriton (IRM) formations, the dolostones of the Lockport Group and the Quaternary overburden with the position of the head loss (H) in boxes. **a** Ca (from Skinner 2019), **b** Cb (from Nunes et al. 2021), and **c** Cc (Nunes et al. 2021)

from 2 to 10 m thick, except in the south and east quadrants where they thicken due to the presence of the Paris-Galt moraines (Arnaud et al. 2018; Priebe et al. 2019, 2021; Nunes et al. 2021), or in localized areas relating to buried bedrock valleys (Steelman et al 2017).

The Lockport Group is described as hydrogeologically heterogeneous, with each formation beneath the city of Guelph typically featuring different matrix and bulk hydraulic conductivities that can be found in Table 1, derived from laboratory measurements of intact core plugs, straddle

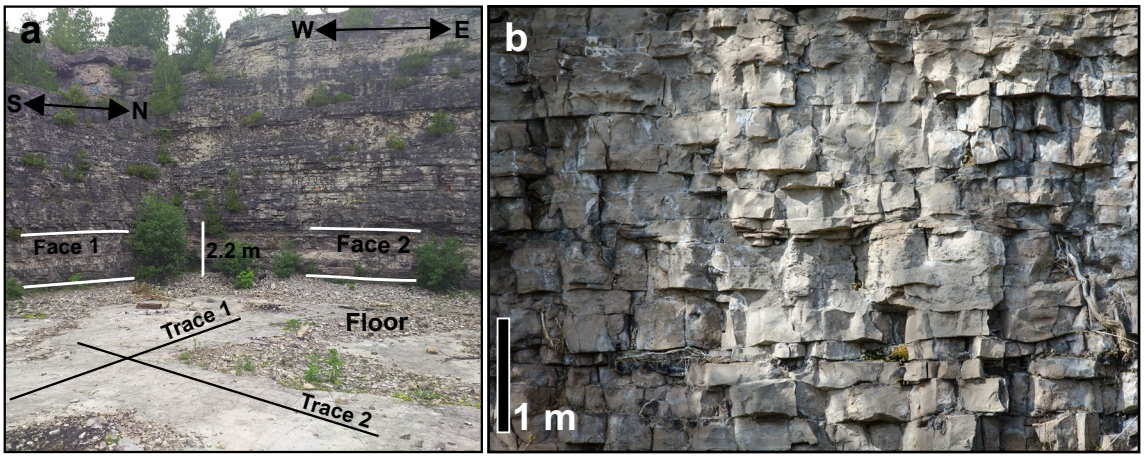

Fig. 3 Photographs of the inactive Reformatory Quarry in Guelph showing the pattern of fracturing within the Eramosa Formation of the Lockport Group. **a** The quarry walls (faces 1 and 2 where the scanlines were performed) and floor, **b** A close-up of face 2 showing bedding parallel fractures and high-angle joints

packer tests, and pumping tests. Values of the 63 core plugs are representative of the rock matrix vertical hydraulic conductivity (K_v), and range three orders of magnitude from 1×10^{-12} to 9×10^{-8} m/s (Skinner 2019; Johnson 2020). These vertical hydraulic conductivity values are highest in the Stone Road and Reformatory Quarry members of the Eramosa Formation (marl-rich samples from the Vinemount Member of the Eramosa Formation were not tested since they were mechanically weak), and followed by the Goat Island, the Guelph, and the Gasport formations, as summarized in Table 1.

The bulk horizontal hydraulic conductivity (K_h) values from straddle packer testing range from 6×10^{-8} to 1×10^{-4} m/s, with the highest values in the Gasport Formation, followed by the Guelph, Eramosa, and the Goat Island formations (Quinn et al. 2011). Similarly, the pumping tests show variability from 4×10^{-6} and 2×10^{-3} m/s across the city of Guelph, with the Gasport Formation being the most conductive geological unit followed by the Guelph, the Eramosa, and the Goat Island formations. The hydraulic conductivity values increase with the observation scale from the core plug, to the packer test interval, and up to the pumping-test scale (Table 1). The lower matrix hydraulic conductivity values relative to the higher hydraulic conductivities of the larger-scale tests support the notion of a fracture-dominated flow system, with little flow through the rock matrix (Maldaner et al. 2019; Munn et al. 2020). The hydraulic conductivity of the Gasport Formation is high according to both packer and pumping tests (Table 1), and represents the main supply aquifer of the city of Guelph, with bulk hydraulic conductivities from pumping test analysis providing a median value of 5.0×10^{-5} m/s. The hydraulic conductivity in the Gasport Formation is high and varies over 2 orders of magnitude according to either straddle packer or pumping tests (Table 1). This variability can be potentially related to the degree of connectivity of fractures, and dissolution enhanced subhorizontal bedding plane fractures that form conduits. Dissolution enhanced matrix porosity is also present in the Gasport Formation. The Guelph Formation is also relatively permeable, and represents the secondary aquifer unit (Skinner 2019; Johnson 2020; Nunes et al. 2021). The Eramosa Formation, comprised of the Vinemount, Reformatory Quarry, and the Stone Road members, rests below the Guelph Formation and is traditionally considered the aquitard unit based on core log and borehole hydraulic testing using packers. When present in the Guelph region, the Vinemount Member averages 10 m in thickness (Brunton and Brintnell 2020). The Goat Island Formation is comprised of the Niagara Falls and Ancaster members. These members have relatively lower hydraulic conductivities according to hydraulic tests performed across the city of Guelph (Table 1), although the Goat Island Formation can have transmissive horizontal fractures (Munn et al. 2020).

Broadly speaking, the aforementioned hydrogeological scenario is characterized by two systems. Water table and potentiometric surface maps indicate that groundwater flow directions in the shallow, sometimes unconfined Guelph Formation mirrors the topography, flowing from high elevations and discharging into rivers and creeks (Priebe et al. 2019, 2021). However, in the deeper Gasport Formation regional flow is south–southwest, but locally flow directions are modified from the city's 21 operational water supply wells (Nunes et al. 2021). The Guelph and the Gasport aquifer units appear to be divided by one or more aquitard units, as seen by multidepth monitoring locations across the city of Guelph (Meyer et al. 2014; Nunes et al. 2021). An intermediate aquitard is thought to protect the lower Gasport Formation aquifer from

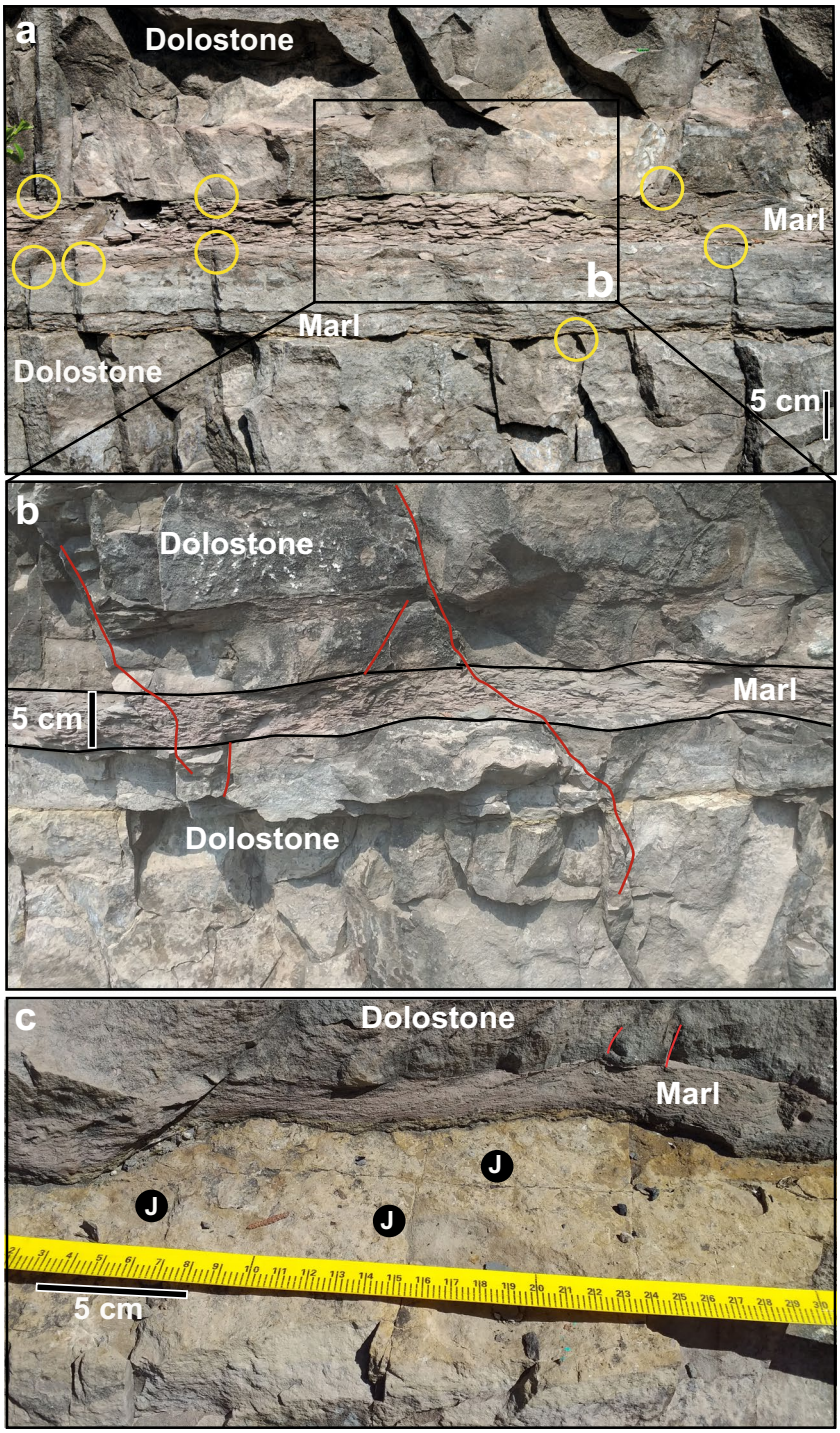

Fig. 4 Marly layers in the Eramosa Formation of the Lockport Group at the Reformatory Quarry, Guelph. **a** Vertical joint terminations (highlighted using yellow circles) in dolostone observed at marl-rich bed contacts, **b** Red trace lines showing refraction through 5-cm thick marl-rich carbonate relative to overlying and underlying dolostone; it is noteworthy that joints can cut marl beds, **c** Red trace lines showing joints (J) terminating at marl contacts

contaminants and has been conventionally assigned to the Vinemount Member. It is well established that the Gasport Formation shows a distinctive hydro-chemical fingerprint at the scale of this study with lower concentrations of sodium and chloride and lower electrical conductivities compared to the shallower Guelph Formation due to road salt applications (Salek et al. 2018; Nunes et al. 2021).

Materials and methods

The Silurian Lockport Group was investigated by studying high-spatial-resolution hydraulic head profiles collected from 24 multilevel monitoring locations across the city of Guelph in vertical boreholes (Fig. 1c). Borehole

geophysical data from 29 vertical and 9 inclined boreholes, with a total linear length of 1,912 m were used to inform lithostratigraphy and fracture distributions (depth and orientations). These data derive from acoustic televiewer, natural gamma (sensitive to clay content and capable of inferring marl-rich beds), and lithological logs collected from continuous rock core samples. In addition, 34 outcrop scanlines were performed to complement the borehole data and to obtain information on high (50–90°) angle fracture length, height, and terminations. These datasets are combined to assess fracture network characteristics associated with the observed inflections in the hydraulic head profiles across the city, which have been used to identify the position of aquitard units. Borehole geophysical logs and hydraulic head profiles were collected from 2006 and 2020 at the various locations shown in Fig. 1 from 2006 to 2020 and listed in Table 2.

Analysis of rock discontinuities

Rock discontinuities (i.e., fractures) were studied in all the bedrock bore and cored holes (Table 2) and the two outcrops

Fig. 5 Pavements showing joint traces in the Vinemount Member of the Eramosa Formation at the Reformatory Quarry

Table 1 Range of values reported for matrix vertical (K_v) from core plugs and bulk horizontal (K_h) hydraulic conductivity from straddle packer testing, and pumping tests within the study area

Geological unit	Matrix K_v (m/s)	Bulk K_h (m/s)	
	Core plug (Skinner 2019)	Straddle packer tests (Quinn et al. 2011; Skinner 2019; Johnson 2020)	Pumping tests (Stantec 2009; Golder 2011; Priebe et al. 2019)
Guelph Formation	3×10^{-10}–3×10^{-9}	1×10^{-5}–9×10^{-5}	9×10^{-6}–3×10^{-4}
Eramosa Formation	5×10^{-10}–9×10^{-8}	4×10^{-7}–2×10^{-5}	2×10^{-5}–3×10^{-5}
Goat Island Formation	3×10^{-10}–6×10^{-9}	6×10^{-8}–3×10^{-7}	4×10^{-6}–9×10^{-6}
Gasport Formation	1×10^{-12}–9×10^{-12}	8×10^{-5}–1×10^{-4}	2×10^{-4}–2×10^{-3}

Table 2 Location, and name for 37 bedrock boreholes characterized using ATV and natural gamma *NA* not applicable

Field site	Boreholes		Logged interval (m)
	Vertical wells	Inclined wells	
North East Guelph	SEN-04, SEN-05, SEN-06, BH-401	NA	230
North West Guelph	MW-367-6	ACH-01, ACH-02, ACH-03	240
Membro	M20, M22, M29	NA	260
Alice Street	BH1, MW1520, MW1521, MW1522, MW1523	NA	252
Scout Camp	SCV1, SCV2, SCV3	SCA1, SCA2, SCA3	244
G360 FRO	GDC-05, GDC-06, GDC-07, GDC-08, GDC-09, GDC-10,	GDC-4, GDC-11, GDC-12	385
South Guelph	Tier3-10[a], GSMW2-09, GSTW1-08[a], GSTW3-08[a], HBP5, MOE/PW/88, VPV-01	NA	301

[a]Wells that have not been cored

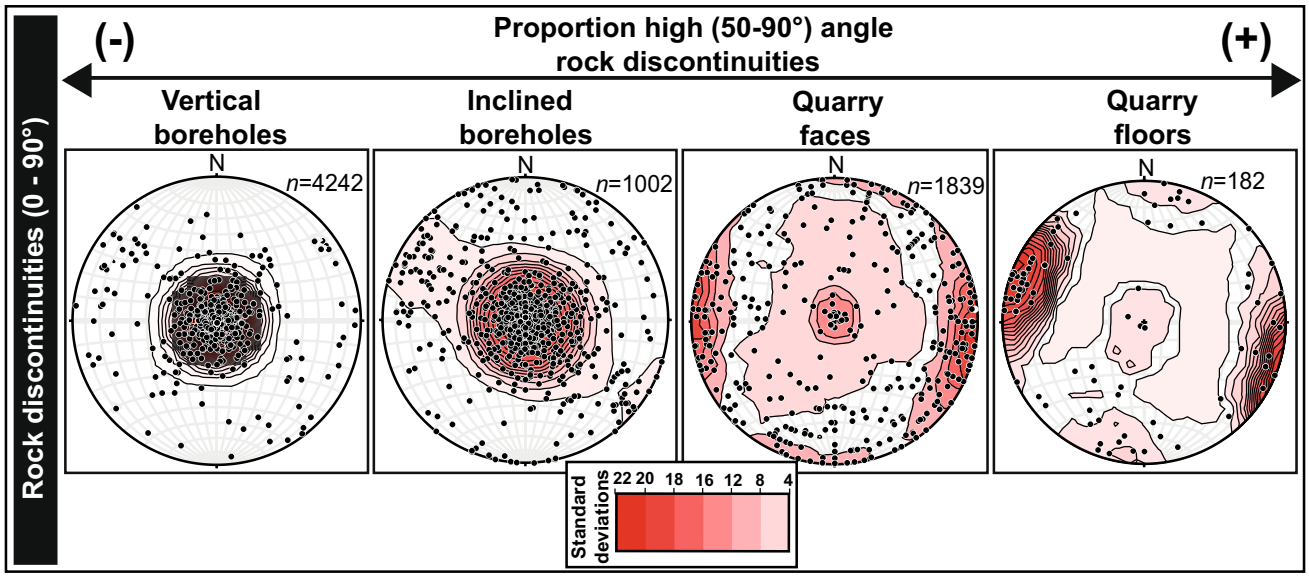

Fig. 6 Summary of the rock discontinuity dataset. Stereonets of poles to planes for fractures with standard deviation of Kamb contours for vertical and inclined boreholes and quarry faces and floors demonstrating the likelihood of each method of sampling high-angle discontinuities

(Fig. 1c). The combination (Fig. 6) of vertical and inclined boreholes as well as scanlines of quarry faces and floors provided a range of sampling orientations to reduce sampling bias (Terzaghi 1965). A previous study at the Guelph site has shown that incorporating fracture data from three inclined boreholes was more effective at sampling high (50–90°) angle joints compared to using vertical boreholes alone (Munn 2012). Overall, in this study, 7,265 rock discontinuities (dipping 0–90°) were logged and plotted in stereonets as poles to planes to support fracture network interpretations and associations with hydraulic properties and head profiles. The total number of rock discontinuities collected in outcrop and in vertical and inclined wells is 4,346, 443, and 2,476 for features dipping 0–35°, 35–50°, and 50–90°, respectively. Contours of poles and Terzaghi (1965) correction were computed with the Stereonet 11 Software that was informed with trend, plunge for each borehole and scanline, and maximum correlation factor (Allmendinger et al. 2012). The statistics of rock discontinuities from outcrop exposures and boreholes are summarized in stereonets (Fig. 6 and Figs. S2 and S3 of the ESM) for dip orientation and inclination, graphs (Figs. 7 and 8), and in tables (Tables 3, 4 and 5) for fracture spacing, heights, length, and stacked bars for summarizing the type of termination. Spacing of high (50° = –90°) angle joints and bed thickness were plotted together in scatter plots to establish a relationship between the two parameters following the method outlined by Rustichelli et al. (2016). The proportion of high-angle joints increases from left to right in Fig. 6, showing results for the vertical boreholes, to the inclined boreholes, and then to the quarry faces and pavements, respectively. Using all data sources, including inclined boreholes and outcrop scanlines, the proportion of low angle (0–35°) discontinuities is 0.6 (4,330 bedding plane fractures divided by the total of 7,265 fractures).

Outcrop scanlines

During June and July of 2021, horizontal scanline surveys were performed at two study sites within the city of Guelph (Fig. 1c)—the Reformatory Quarry (Figs. 3a,b, 4a–c and 5a and Figs. S1a and S1b of the ESM), and the Barber Scout Camp (Fig. S1c also of the ESM)— and fracture data was collected from quarry faces ($n = 1{,}839$) and pavements ($n = 182$), respectively. The Reformatory Quarry is the type-section for the Reformatory Quarry Member of the Eramosa Formation, with this member making up the majority of the quarry wall exposures. The lower few meters of the wall expose the Vinemount Member (Eramosa Formation) and the upper few meters expose the Guelph Formation (Brunton and Brintnell 2020). The Barber Scout Camp location (Fig. S1c of the ESM) is adjacent to a bedrock river with exposed marls of the Vinemount Member of the Eramosa Formation on the ground surface. Thirty horizontal scanlines with a 10-m length were collected on faces 1 and 2 at the Reformatory Quarry (the beds where scanlines were performed are illustrated in Fig. 3a with white lines on the two rock walls). On each quarry face, 10 scanlines were conducted on dolostone beds (Fig. 2a–c), and 5 on marl beds (Fig. 3a,b, and Fig. S1a of the ESM). The two rock faces are nearly orthogonal and oriented NNE–SSW and WNW–ESE. The thickness of the thirty beds where the scanlines were performed was also recorded.

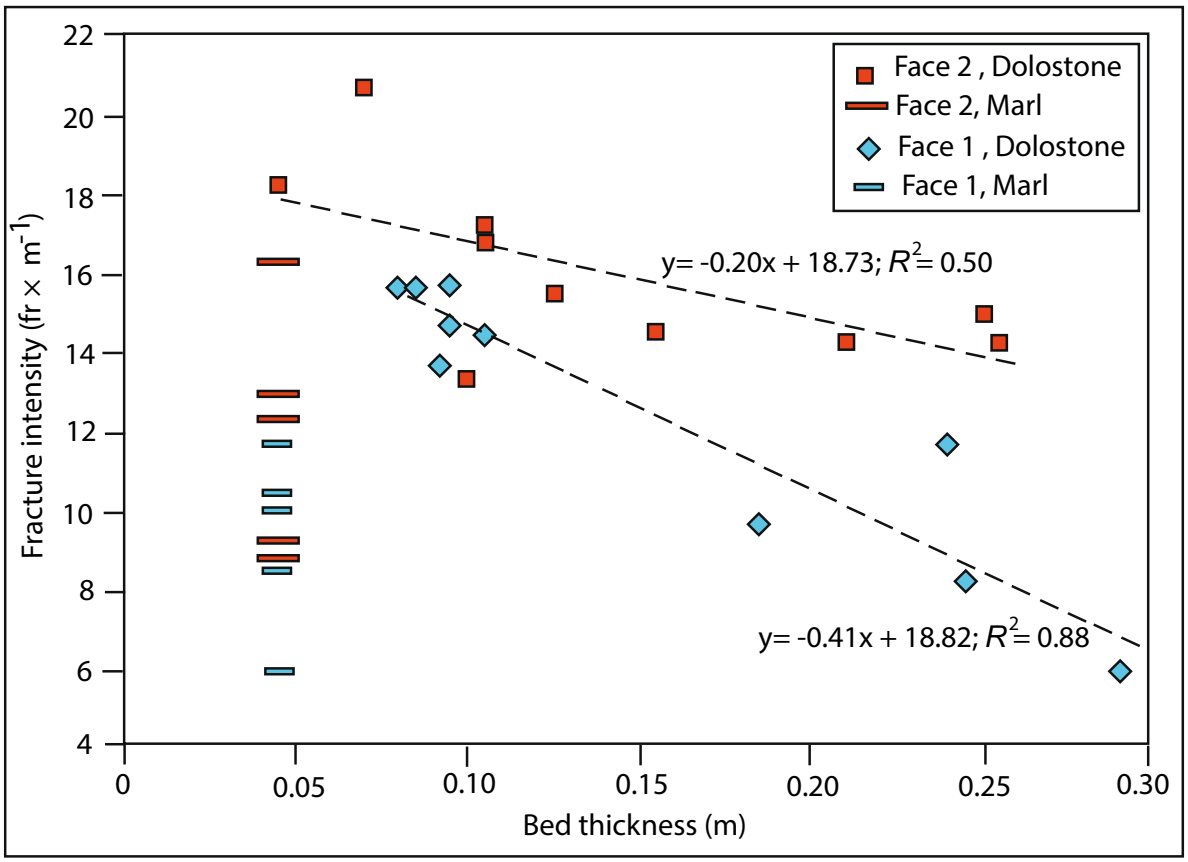

Fig. 7 Scatter plot of bed-thickness vs. fracture intensity at Reformatory Quarry (see Fig. 1c for location) in the Eramosa Formation acquired along face 1 (NNW–SSE) and face 2 (ESE–WNW)

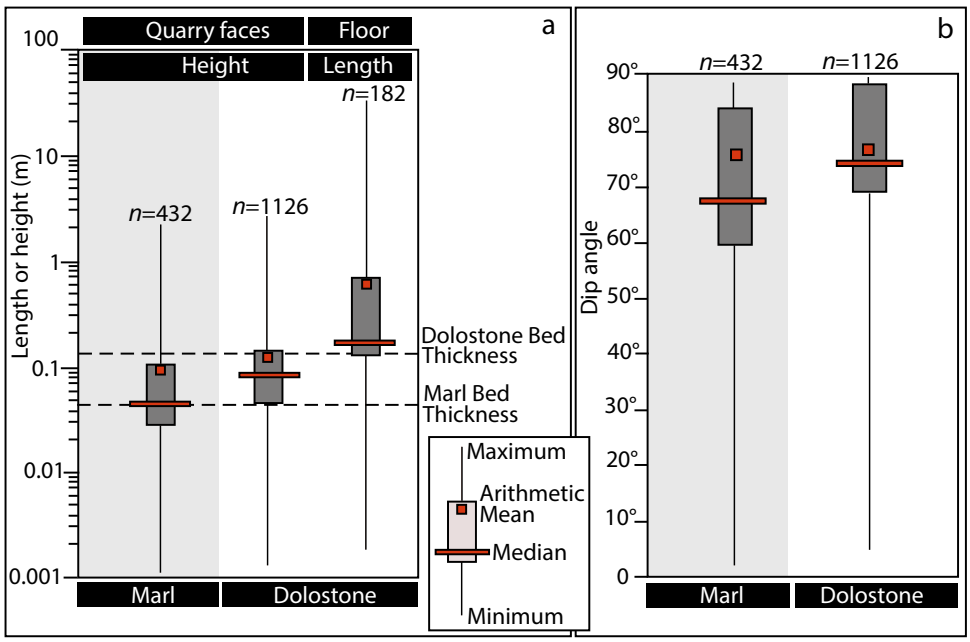

Fig. 8 Statistics on the geometry of rock discontinuities at Reformatory Quarry (see Fig. 1c for location) in the Eramosa Formation acquired along face 1 (NNW–SSE) and face 2 (ESE–WNW) and the pavements of either the Reformatory Quarry or the Barber Scout Camp. **a** Box plots of **a** Persistence of joints at quarry faces and pavements in marl and dolostone, **b** Statistics on dip angle in marl and dolostone acquired on vertical rock faces

Table 3 Location and length of scanlines, and statistics of rock discontinuities

Location	Scanline group	Number of scan lines	Cumulative scanline length (m)	*n* rock discontinuities	Rock type	Orientation scanline	Average length (cm)	Average spacing (cm)
Reformatory Quarry	Face 1	10	40	488	Dolostone	NNE–SSW	13.3	7.8
	Face 2	10	40	638	Dolostone	WNW–ESE	10.8	7.8
	Face 1	5	40	203	Marl	NNE–SSW	8.12	9.9
	Face 2	5	40	229	Marl	WNW–ESE	9.4	8.8
	Line 1, floor	1	3.5	35	Dolostone	NNE–SSW	107.6	8.5
	Line 2, floor	1	3.5	41	Dolostone	WNW–ESE	66.1	10.1
Scout Camp	Line 1, floor	1	3.5	50	Dolostone	NNE–SSW	27.1	5.2
	Line 2, floor	1	3.5	52	Dolostone	WNW–ESE	42.5	5.0

Table 4 Length of interval logged in the boreholes in Table 2 and frequency of low and high-angle joints in ATV logs in the formations and members of the Lockport Group

Geological formation	Geological member	Length of borehole interval logged (m)	Linear fracture intensity, P10 mean, fractures (fr) × m^{-1}	
			High-angle discontinuities (50–90°)	Low-angle discontinuities (0–15°)
Guelph Formation	Hanlon Member	250	0.21	3.0
Guelph Formation	Wellington Member	288	0.19	2.0
Eramosa Formation	Reformatory Quarry Member	100	0.20	3.3
	Vinemount Member	137	0.42	3.6
Goat Island Formation	Ancaster Member	166	0.05	5.5
	Niagara Falls Member	100	0.16	4.8
Gasport Formation	N/A	709	0.28	1.2

The scanline logging method (Hitchmough et al. 2007) included recording five parameters—dip direction and inclination, fracture spacing, fracture trace persistence (heights on quarry walls, and length on pavements), and bed thickness. The type of fracture termination was also recorded adding a new and sixth observation to the traditional guidelines used for scanline surveys. Fracture termination represents the geometrical relation of a high (50–90°) angle joint relative to the bedding planes at the top and bottom that form a mechanical unit. A bedding plane discontinuity is a low-angle (0–35°) discontinuity mechanically open that either divides two adjacent dolostone layers or a dolostone from a marly layer. The definition of bedding plane discontinuity is mechanical with no conceptual link with sequence stratigraphy.

The fracture terminations were categorized into nine types and four groups (Fig. 9a). Type 1 (or group a, Ga) represents a joint confined in the bed with no mechanical contact with the bedding plane at the top and bottom. Types 2 and 3 represent joints that touch the bedding discontinuities exclusively at the top or bottom, respectively. Types 4 and 5 are joints that crosscut bedding discontinuities exclusively at the top and bottom, respectively. Note that types 2–5 forming group b (Gb) are characterized by joints with a single mechanical contact with the bedding plane fractures. Type 6 contacts the bedding plane at the bottom and crosscuts type 1 at the top. Type 7 crosscuts the bedding plane at the bottom and touches type 1 at the top. Type 8 touches both the bounding bedding planes discontinuities and is confined by the bedding planes. Types 6–8 characterize group c (Gc), which is characterized by joints with two mechanical contacts with bedding plane fractures and is partially confined by the bedding planes. Type 9, or group d (Gd), crosscuts the bedding plane discontinuities at the top and bottom with no confinement by the mechanical units (Fig. 9a). Thus, moving from Ga to Gd, the joints are characterized by a higher number of mechanical connections between the joint and bedding planes. This degree of connection between joints and bedding planes is called mechanical connectivity since no direct and quantitative information on hydraulic connectivity can be collected by performing scanline surveys in the field.

Table 5 Statistics of fracture intensity from the nine inclined wells (SCA1, SCA2, SCA3, ACH-01, ACH-02, ACH-03, GDC-4, GDC-11, GDC-12) logged at the study site. Data were collected from the Barber Scout Camp, North-West Guelph and G360FRO where 324, 647 and 526 fractures were detected by ATV, respectively. *NA* indicates lithostratigraphic unit not present in borehole dataset from the site. *m.s.d.* mean standard deviation

Lithostratigraphy		Scout Camp (SCA1, SCA2, SCA3)			North-West Guelph (ACH-01, ACH-02, ACH-03)			G360FRO (GDC-4, GDC-11, GDC-12)		
Geological Formation	Geological Member	Linear fracture intensity, P10 mean, fractures (fr) × m^{-1} (m.s.d., vertical spacing)		Length of borehole interval logged (m)	Linear fracture intensity, P10 mean, fractures (fr) × m^{-1} (m.s.d., vertical spacing)		Length of borehole interval logged (m)	Linear fracture intensity, P10 mean, fractures (fr) × m^{-1} (m.s.d., vertical spacing)		Length of borehole interval logged (m)
		0–35°	50–90°		0–35°	50–90°		0–35°	50–90°	
Guelph Formation	Hanlon	NA	NA	0	NA	NA	0	NA	NA	0
	Wellington	NA	NA	0	1.62 (0.4)	0.75 (5.3)	100	NA	NA	0
Eramosa Formation	Stone Road	NA	NA	0	NA	NA	0	NA	NA	0
	Reformatory Quarry	NA	NA	0	NA	NA	0	3.77 (0.2)	0.27 (0.5)	56
	Vinemount	8.24 (0.14)	0.93 (1.0)	20	NA	NA	0	4.25 (0.1)	0.40 (0.7)	50
Goat Island Formation	Ancaster	1.33 (0.2)	0.10 (1.1)	20	NA	NA	0	3.25 (0.2)	0.06 (1.2)	56
	Niagara Falls	NA	NA	0	NA	NA	0	3.73 (0.2)	0.4 (1.0)	60
Gasport Formation		1.50 (0.3)	0.12 (5.2)	37	1.46 (0.6)	0.53 (1.0)	222	1.42 (0.5)	0.17 (1.8)	100

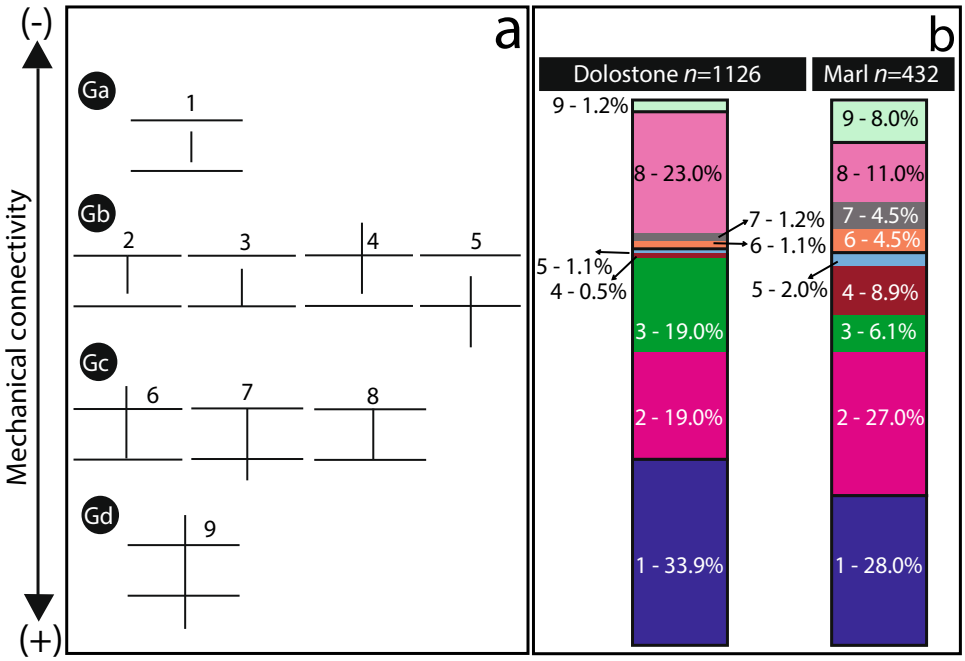

Fig. 9 Statistics on the nine types of terminations (1–9) and four groups (Ga, Gb, Gc, and Gd) for the high-angle joints of the Eramosa Formation at the Reformatory Quarry for either marls or dolostones. **a** Scheme, **b** Data summary

Excellent outcrop exposures on the ground at both the Reformatory Quarry and Barber Scout Camp allowed for the measurement of dip direction and angle, persistence and spacing of fractures and bedding planes using horizontal scanlines. At these two sites, horizontal scanlines of 3.5 m in length were performed on the ground pavements (Figs. 3a and 5a and Fig. S1c of the ESM) along both WNW–ESE and NNE–SSW orientations. Measurements were collected from rock faces (faces 1 and 2 in Fig. 3a) or pavement (traces 1 and 2 in Fig. 3a) at the Reformatory Quarry. No rock walls were exposed at the Barber Scout Camp. Here, structural data were recorded exclusively from the ground pavement (Fig. S1c of the ESM), and therefore no information on the thickness of the beds was collected. The fractures intersecting the pavements provided a three-dimensional (3D) perspective due to differential erosion that is sufficient for estimating the dip angle for the lithologies in exposure at the Reformatory Quarry and Barber Scout Camp.

Bedrock borehole geophysics

Acoustic Televiewer (ATV) and natural gamma logs were performed using ALT ABI-40 and Mount Sopris 2PGA probes, respectively. The ATV was logged using a low speed (1.2–1.5 m min^{-1}) to achieve accurate and high-quality image data. The quality of the ATV was also high due to the fact that 92% of the studied wells (36 out of 39) were cored holes with relatively smooth borehole walls, making the contrast between fractures and borehole walls more apparent (Table 2). Depth, dip angle, and direction of rock discontinuities were recorded from structure picking (Williams and Johnson 2004) of the acoustic televiewer images in vertical and inclined boreholes that plunge 60° from horizontal (Fig. 1c; Table 2). This analysis was conducted in WellCAD Software Version 5.6 and all the open discontinuities characterized by low acoustic amplitude and travel time were picked using the software. In the inclined borehole datasets, the structure logs were corrected to account for the intersection angles between the fracture and boreholes, such that the fracture dip direction and angle reflected the true orientation and not the apparent orientation in the borehole images. Corrections for magnetic declination were also conducted for all borehole image logs. Orientation of rock discontinuities ($n=5244$) was represented using stereonets as explained previously. Statistics on the vertical spacing of low (0–35°) and high (50–90°) angle discontinuities were organized according to the updated lithostratigraphic nomenclature recently proposed by Brunton and Brintnell (2020). It is noteworthy that the precision in the position of the lithostratigraphic unit boundaries in continental and shallow water carbonates such as the dolostones of the Lockport Group are subject to uncertainties due to (1) gradational contacts or interfingering between units, and (2) lateral variation of the combination of lithofacies that characterize either geological members or formations (Carannante et al. 1988; Mancini et al. 2021). The range of 0–35° represents the range of the bedding planes, bedding parallel and cross-bedded laminations of sedimentary origin that have been mechanically reactivated at the study site (Brunton and Brintnell 2020). This 0–35° category of rock discontinuities includes both bedding fractures and stylolites. The stylolites make up 8 and 5% of the acoustic televiewer and outcrop datasets, respectively. Issues

of resolution of acoustic televiewer logging and weathering on outcrop surface may have reduced the proportion of measured stylolites relative to the actual number. Joints dipping from 35 to 50° were rare, accounting for only a small proportion (<2%) of the borehole data. The small number of medium angle fractures did not allow comparison of the moderately (35–50°) dipping joints with the different lithostratigraphic units. However, these moderately (35–50°) dipping fractures were incorporated into the stereonets. The lower cut-off angle (50°) for the high-angle (≤90°) joints was chosen based on the presence of extension-related tectonic fractures that are generally dipping 60°, but can have a lower angle due to the presence of mechanically weak marls (Underwood et al. 2003).

Hydraulic head characterization

Vertical hydraulic head profiles

The magnitude and position of the head loss were assessed in 24 boreholes containing multilevel monitoring infrastructure (Fig. 1b) across the city of Guelph, obtained from the MG360 database. These data have been summarized in Table 6 and Fig. S4 of the ESM, and the hydraulic head profiles previously published have been referenced accordingly. High-resolution, engineered multilevel systems (MLS) with many depth-discrete ports, and temporary deployment (TD)—e.g., Pehme et al. (2014); Capes et al. (2018)—were all used in the study to measure the hydraulic head in discrete intervals. Specific information on the number of monitoring intervals and the range in monitoring interval lengths relative to borehole length are provided for each borehole in Table 6. In this study, TD systems provide the highest spatial resolution, with a total of 187 monitoring intervals over 471 m of vertical borehole distance (0.40 ports per meter on average), followed by the Westbay™ multilevel, which totaled 189 monitoring intervals over 525 m of vertical distance (0.36 ports per meter on average), the G360 Multi Port System and Modified Solinst Waterloo System totaled 39 monitoring intervals over a 261-m-vertical distance (0.15 ports per meter on average), and the Water FLUTe™ system totaled 28 monitoring intervals over 190 m of vertical distance (0.15 ports per meter on average). The TD systems utilize a single small-diameter nylon-coated braided steel cable with multiple pressure transducers attached (in this case, RBRsoloD or RBRduetT.D), which are installed in a borehole to target specific features and fractures and subsequently sealed in the borehole using a blank FLUTe™ liner described further by Cherry et al. (2007). The MG360, modified Waterloo Solinst and Westbay™ commercially available multiport monitoring systems are composed of segmented sections of casing and measuring ports configured to target specific depth intervals. Such systems are completed with either packers to provide seals between ports or backfilled with inert sand around the port/monitoring intervals and the seals between ports are created using granular or pelletized bentonite (Parker et al. 2006).

Of note, six borehole locations (Table 6) were selected between the 24 locations described in the preceding for comparison of the hydraulic head profile with fracture orientations obtained from ATV logs, and natural gamma, rock core, or OTV logs providing context for the lithostratigraphy. The selection is based on the high vertical resolution (Table 6) of the six wells (GSMW2-09, VPV-01, SEN-07, SEN-05, Tier3-10, and MW367-6), and availability of both ATV logs and natural gamma ray to assess the role of fracture characteristics and marl-rich zones on head loss occurrence. The six selected wells are distributed across the 95-km^2 study area to represent different quadrants of the city of Guelph (Fig. 1b).

Vertical component of hydraulic head gradients

The depth-discrete head data from the MLSs were used to calculate the vertical component of hydraulic gradient (i_v) between adjacent monitoring zones using Eq. (1) for the six wells highlighted in Fig. S4 of the ESM and Table 6.

$$i_v = \frac{(h_2 - h_1)}{L} \tag{1}$$

where h_1 is the head in the shallower port, h_2 is the head in the deeper port, and L is the length of the seal over which the change in head occurs. Using this convention, a negative value indicates a vertical component of gradient that would generate downward flow. Calculating the vertical gradient across the length of the seal provides the maximum vertical gradient based on the well construction that best represents field conditions, provided that blending of head within ports is minimal (Meyer et al. 2014).

Results

Fracture network

Outcrop

Scanline surveys were performed on rock walls and pavements to collect a higher proportion of high-angle joints relative to the vertical and inclined boreholes (i.e., reducing sampling bias). Data collected on pavements almost exclusively sampled high-angle joints (see contouring of pole to planes in Fig. 6). High (12–22) and low (4–12) values of standard deviations of Kamb contours of poles to planes characterize high (50–90°) and low (0–35°) angle fractures,

Table 6 Multilevel monitoring system details, hydraulic head data, and stratigraphy of the 24 boreholes extracted from the MG360 database. The stratigraphic locations of head loss occurrence are shown with "*x*" marks. *Fm* Formation, *Mbr* Member

BoreholeID	MLS type	Length of bedrock interval (m)	No. of ports	Vertical port length range (m)	Hydraulic head (m)			Head loss occurrence by Lockport Group lithostratigraphy									Reference
					Min	Max	Δ	Guelph Fm		Eramosa Fm			Goat Island Fm		Gasport Fm		
								Hanlon Mbr	Wellington Mbr	Stone Road Mbr	Reform. Quarry Mbr	Vinemount Mbr	Amcaster Mbr	Niagara Falls Mbr	Upper (0 – 8 m)	Lower	
BH-401	Water FLUTe	67.1	10	1.59–5.34	314.41	320.85	–6.44				x	x	x				Nunes et al. 2021
GDC-05	Temporary deployment	53.62	32	0.45	313.88	310.68	–3.20				x	x	x	x			Maldaner et al. 2018
GDC-12	Temporary deployment	52.67	19	0.43	319.22	323.40	–4.18				x	x	x	x			Munn et al. 2020
GSMW9	Temporary deployment	51.0	25	0.4–1.2	333.66	313.91	–19.75					x	x	x	x		This study
HPB5	Temporary packer string	70.75	27	1.53	297.35	323.10	–25.75				x	x	x				Stockford 2023
MW-24	Westbay	98.1	40	0.6–4.3	336.6	340.4	–3.83	x									Meyer et al. 2014
MW3676	Westbay	97.14	45	0.61–4.27	337	340	–3.0	x									This study
SEN-01	Solinst Waterloo	64.5	7	1.4–6	295.5	311.5	–16.0				x				x		Johnson 2020
SEN-02	Temporary deployment	56.1	18	0.3–0.6	286	289	–2.7				x	x	x	x	x		Johnson 2020
SEN-03	Temporary deployment	59.26	21	0.28–0.6	293	301	–8.2					x			x		Johnson 2020
SEN-04	Solinst Waterloo	32.1	7	1.2–3.5	308.17	326.04	–17.87		x	x	x		x				Skinner 2019

Table 6 (continued)

BoreholeID	MLS type	Length of bedrock interval (m)	No. of ports	Vertical port length range (m)	Hydraulic head (m)			Head loss occurrence by Lockport Group lithostratigraphy									Reference
					Min	Max	Δ	Guelph Fm		Eramosa Fm			Goat Island Fm		Gasport Fm		
								Hanlon Mbr	Wellington Mbr	Stone Road Mbr	Reform. Quarry Mbr	Vinemount Mbr	Amcaster Mbr	Niagara Falls Mbr	Upper (0 – 8 m)	Lower	
SEN-05	Temporary deployment	68.21	23	0.3–0.6	321.72	332.77	–11.05				x	x	x				This study
SEN-06	Temporary deployment	62.6	25	0.3–0.6	320.04	332.82	–12.78				x		x	x	x		Skinner 2019
SEN-07	Temporary deployment	67.48	24	0.35–0.7	303.69	315.36	–11.67					x	x		x		This study
SEN-08	G360 MPS	58.09	8	1.4–3.07	295	302.2	–7.2				x	x	x		x		Johnson 2020
Tier3-01	Solinst Waterloo	85.95	9	1.8–5.0	335.9	338.5	2.6				x		x	x			Unonious 2012
Tier3-07	Water FLUTe	63.1	9	1.2–4.0	341	353	–12.0					x	x				Unonious 2012
Tier3-08	Water FLUTe	60.2	9	1.6–4.7	333	342	–9.0					x	x				Unonious 2012
Tier3-09	Westbay	59.1	15	1.5–4.3	326	340	–14.0						x				Nunes et al. 2021
Tier3-10	Westbay	66.9	17	1.52–3.5	302.56	320.97	–18.41						x	x			This study
M20	Solinst Waterloo	20.56	8	0.61–1.28	313.27	313.97	–0.3				x	x					Fernandes 2017
UG-01	Westbay	72.8	26	0.61–3.66	328.08	336.01	–7.93					x	x				Leite 2015
VE-01	Westbay	59.56	23	0.61–3.35	326.29	326.45	–0.16					x	x	x			Leite 2015
VPV-01	Westbay	71.18	23	0.6–4.08	328.93	330.15	–1.22					x	x	x	x		This study

respectively, for the quarry floors (Fig. 6). The data collected on the rock faces also shows that the intensity of the high-angle joints decreases with increasing thickness of the dolostone beds on both face 1 (striking 15–195°) and face 2 (striking 105–285°) at the Reformatory Quarry (Fig. 7). The marl beds had a more uniform thickness (4.7–5.2 cm) on both the rock faces and, therefore, a correlation between bed thickness and fracture intensity could not be conducted within this lithology. The arithmetic average thickness of the marl-rich and dolostone beds is 5 and 11 cm, respectively (Fig. 7). Such thin beds of dolostones and marls overlap in terms of fracture frequency according to outcrop scanlines performed on vertical rock faces (Fig. 7).

These thicknesses fit the interquartile range of high-angle joint heights collected on the quarry walls for the two lithotypes (Fig. 8a). Length of high-angle joints measured on the pavements is much larger than the heights. The lengths of the joints on the pavement range from 0.01 to 20 m with median and arithmetic averages of 0.2 and 0.8 m, respectively, as shown in the box plot in Fig. 8a and Table 3. Joints are characterized by lower height in marls relative to the dolostones by comparing the minimum, median, arithmetic average and maximum joint length between the two rock types (Fig. 8a). The maximum joint height of marls is 2.0 m, and slightly larger at 2.2 m for the dolostones (Fig. 8a). These relatively long joints that cross-cut the bedding planes can occur in clusters and are vertically parallel with a height of 1.5–2.2 m. There are also corridors of subvertical fractures that are ≤6 m long (Fig. 3c). These very long structures (≤6 m in length) have been sampled on vertical quarry faces in scanline surveys in the southern part of face 1 (Fig. 3a). Detailed examination of the outcrop shows that these structures are comprised of multiple distinctive joints (1–2.2 m long) that are disconnected with distinctive terminations (Fig. 3c,d), which is the reason for a maximum of 2.2 m for the joint height on the vertical faces at the study site. Overall, a joint of 2 m can intersect 40 beds that are 0.05 m thick in marls. A 2.2-m thick joint is a cutoff that can intersect 14.6 beds that are 0.15 m thick according to the arithmetic averages.

Notably, joint dip angles are shallower in marls than in dolostone beds, as can be observed by comparing maximum, minimum, median, arithmetic mean, and the 25th and 75th percentiles of the dip angle (Fig. 8b). The dip angle appears to refract at the bounding surface between marl and dolostone as observed in the outcrop and shown in Fig. 3b, with shallower dip angles in the marls relative to the dolostones (Fig. 8b).

High-angle joints do not crosscut beds in the majority (78.4%) of the measurements at the Reformatory Quarry (Fig. 3a,b). This pattern of rock discontinuities is consistent with a stratabound fracturing system (Odling et al. 1999) where the joints do not crosscut the strata. This scenario is considered an end member in rock mechanics. High-angle joints confined (types 1, 2, 3, and 8) or partially confined within a mechanical unit (types 4–7) together form the groups Ga, Gb, and Gc; and represent the 98.8 and 92.0% in dolostone and marl beds, respectively (see scheme of termination types in Fig. 9b). In all, 27.9 and 5.1% of these joints (termination types 4–7 and 9, respectively) crosscut at least one bedding plane discontinuity in marly and dolostone beds, respectively. These joints (types 4–7 and 9) vertically connect bedding plane discontinuities from a mechanical point of view (Figs. 3a,b, 4a,b and 9b). In marl beds, 8.0% of joints crosscut the mechanical unit at both the top and bottom (terminations nine or group four), an arrangement that decreases to 1.2% in the dolostone beds. Whichever combination of termination types or groups of joints is chosen, the statistics show a higher degree of mechanical connectivity for the marl relative to the dolostone beds (Fig. 9a,b). The marls are, therefore, more thinly bedded (Fig. 8a), have shallower dipping joints (Fig. 8b), are equally intensively fractured as dolostones and more mechanically connective in terms of termination type relative to the dolostones (Fig. 9b).

Overall, the scanlines at the Reformatory Quarry show: (1) high-angle joints with an inverse correlation between frequency of occurrence and bed-thickness for the dolostone beds (Fig. 7); (2) a fit between the thickness of the beds and the height of joints for either marls or dolostones (see values of percentiles for joint heights and arithmetic average of bed thickness in Fig. 8a); and (3) the majority of the joints are confined within the mechanical unit/bed (Fig. 9a,b). The analysis of rock discontinuities on rock faces and floors shows that the high-angle joints include two principal sets that are NNE–SSW and WNW–ESE striking. The dominant direction of the high-angle joints is NNE–SSW at both the pavement of the Scout Camp, and the pavement and walls at the Reformatory Quarry. The length of the joints striking NNE–SSW measured on the pavement is slightly higher than the WNW–ESE set, with a median joint length of 1.07 and 0.66 m, respectively (Table 3).

Boreholes

Dip angle and direction of rock discontinuities across the city of Guelph were analyzed using acoustic televiewer logs (Fig. 1c; Table 4). The inclined boreholes have on average a 20% proportion of high (50–90°) angle discontinuities. In the vertical boreholes, this proportion is lower at only 6%, demonstrating the negative bias towards vertical features (Fig. 6). The high-angle joint orientations typically contain two principal sets, with one being dominant at each site, though the directions of the two sets vary somewhat across the study area (Figs. S2a and S3 of the ESM). Notably, the dominant direction of the high-angle joints at each site remains relatively consistent across different lithostratigraphic units (Fig. S2b of the ESM); and

comparing vertical with inclined boreholes at the Barber Scout Camp, MG360 Fractured Rock Observatory (FRO), and Northwest Guelph sites (Fig. S2c of the ESM). The Fisher Mean Vector of all the high-angle joints throughout the city of Guelph in boreholes is striking 336° and dipping 65° WSW.

The Lockport Group contains frequent bedding plane discontinuities with a mean linear fracture (number of fractures defined with the acronym "fr" in the text, figures and tables) frequency of 3.42 fr × m^{-1}; and varies between different lithostratigraphic units. The Guelph and Gasport formations have a lower average vertical frequency of bedding plane discontinuities of 2.1 and 1.2 fr × m^{-1}, respectively (Table 4). The Goat Island and Eramosa formations are more thinly bedded with an average of frequency of bedding plane discontinuities of 5.15 and 3.45 fr × m^{-1}, respectively. In terms of geological members, the intensity of the bedding plane discontinuities is the highest in the Ancaster (5.5 fr × m^{-1}) and Niagara Falls (4.8 fr × m^{-1}) members of the Goat Island Formation, followed by the Vinemount (3.6 fr × m^{-1}) and the Reformatory Quarry (3.2 fr × m^{-1}) members (Table 4). The dip of the bedding plane discontinuities ranges from 0 to 35°; although 95% of these discontinuities dip less than 5°.

The intensity of high-angle joints is the highest in the Vinemount Member of the Eramosa Formation (arithmetic mean = 0.42 fr × m^{-1}). Very low intensity of high-angle joints occurs in the Ancaster Member of the Goat Island Formation (arithmetic mean = 0.05 fr × m^{-1}) in all the seven study sites (North-East Guelph, North-West Guelph, Membro, Alice Street, Barber Scout Camp, G360FRO, and South Guelph) that were studied in the city of Guelph (Table 4). All the other members of the Lockport Group contain similar average values of high-angle joint intensity that range from 0.16 to 0.23 m^{-1} (Table 4).

Overall, the Gasport Formation appears to represent an end member with more massive strata of crinoidal grainstones. The marl-rich Vinemount Member of the Eramosa Formation contains a high intensity of the high-angle joints, and the Ancaster Member of the Goat Island Formation has the lowest intensity of high-angle joints, representing another end member within the Silurian Lockport Group (Table 4). It is noteworthy that restricting the dataset exclusively to inclined boreholes would increase the proportion of high-angle joints by removing bias (Fig. 6). The Ancaster Member has the lowest high (50–90°) angle joint intensity in the inclined wells of North-West Guelph, Barber Scout Camp and G360FRO (Table 5). In these three sites, the Ancaster Member also has the highest bedding plane fracture intensity in the Lockport Group. The intensity of the bedding planes (dipping 0–35°) is the lowest in the Gasport Formation in each location where the inclined wells were drilled (Table 5).

These data demonstrate that joints are organized in two orthogonal principal sets and the dominant direction of the high-angle joints is NNE–SSW at both the pavement of the Barber Scout Camp, and the pavement and walls at the Reformatory Quarry. The two sites are adjacent and show a fit between outcrop and boreholes in terms of the pattern of the fractures (Fig. S3 of the ESM). To help explain the occurrence of head loss observed across the city of Guelph, the statistics of rock discontinuities summarized in Tables 4 and 5 also allow comparison with the detailed profiles of hydraulic head.

Hydraulic head characterization

Position of the head loss

Vertical profiles of hydraulic head from 24 locations across the study area were examined to assess head loss that suggests the presence of low K_v zones or aquitards. The head profiles and nature of head loss were variable and sometimes occurred across multiple members (≤five) and formations (≤three) in the same borehole (Table 6). The head loss was observed to occur in all the geological formations and members of the Lockport Group. Specifically, the head loss was measured in the Gasport Formation (33.3% of the boreholes), Niagara Falls (37.5% of the boreholes) and Ancaster (75.0% of the boreholes) members of the Goat Island Formation, Vinemount (62.5% of the boreholes), Reformatory Quarry (50.0% of the boreholes) and Stone Road (4.2% of the boreholes) members of the Eramosa Formation, Wellington (4.2% of the boreholes) and Hanlon (8.3% of the boreholes) members of the Guelph Formation (Table 6).

Overall, the head loss was most frequently measured in the Ancaster Member of the Goat Island Formation. A head loss rarely occurred in the Wellington Member of the Guelph Formation and is absent in the Lower Gasport Formation (<8 m into this geological formation). It is important to note that, due to erosion and disconformities, all formations and members are not always distinguishable or present at each borehole location. Including only the boreholes where the Vinemount and Ancaster members are observed, head loss in these members occurs in 94 and 86% of boreholes, respectively. While this supports the conventional thought that the Vinemount is a regional aquitard, the head loss typically does not occur across the full thickness of the unit, and in many cases, the majority of the head loss is observed in other members. This scenario highlights the potential importance of the other members of the Lockport Group for providing resistance to vertical flow providing protection to the underlying Gasport Aquifer and refracting flow lines impacting flow trajectories.

Vertical hydraulic head profiles with wireline logs

Contrasts in K_v in different layers often result in inflections in the hydraulic head profile (Meyer et al. 2008) and, in the Guelph area, the vertical component of the gradient is predominantly downward. This scenario portrays a loss of head with depth across the lower K_v layers because of lower head values in the Gasport Formation due to high transmissivities and active pumping. The Goat Island and Eramosa formations are characterized by lower bulk (horizontal) hydraulic conductivities according to straddle packer testing through a comparison with the hydraulic conductivity of the Guelph and Gasport formations (Table 1). The Goat Island and the Eramosa formations can also be discontinuous, interfingered, stacked, or can laterally vary in thickness across the city of Guelph, as shown by the geological cross section (Fig. 2b). Overall, the system of aquitards beneath the city of Guelph is complex due to variations in disconformities and fracture connectivity within the geological formations, resulting in highly variable vertical hydraulic conductivity distributions. Figure 10 provides examples of this geological and hydraulic variability using six selected boreholes across the city of Guelph study area (refer to map in Fig. 1c): three boreholes (GSMW2-09, VPV-01 and Tier3-10) located in the southern part of the city of Guelph, a fourth borehole (SEN-07) located in the central part of the City, and a fifth and sixth (SEN-05 and MW367-8) located in the northern sector of the study site.

A TD system with multiple transducers attached at different depths along a cable is sealed in a borehole using a FLUTe™ liner in GSMW2-09 in the southern part of the study area (Fig. 10a). GSMW2-09 indicates 19.8 m of head loss between the top and bottom of the monitored interval (Guelph Formation to the upper Gasport Formation), with the head profile flattening out in the lower part of the Gasport Formation where it is well connected hydraulically (Fig. 10a). In all, 23% of the head loss occurs in the uppermost Gasport Formation (4.5 m), 59% in the Ancaster and Niagara Falls members of the Goat Island Formation (11.7 m), and 18% in the Vinemount Member (3.6 m) of the Eramosa Formation. High values (≤70 cps) of natural gamma suggest the presence of marls in the Vinemount Member that occur above the depth interval where the hydraulic head reduces. The full interval (273–253 meters above sea level, masl) where the head loss occurs is relatively less fractured (fracture intensity < 1.5 0 fr × m^{-1}) than the rock sequence at the bottom (fracture intensity > 1.5 0 fr × m^{-1}) in the Gasport Formation (246–253 masl), and at the top (fracture intensity > 2.0 fr × m^{-1}) in the Guelph and upper Eramosa formations (273–300 masl). Specifically, a 2-m interval (265–263 masl) in the lower Ancaster Member has no high-angle joints and bedding plane fractures, according to acoustic televiewer data and low (<20 cps) gamma-ray values, suggest no marl beds. This 2-m-thick interval is interbedded between intervals with P10 for high-angle joints of 1 fr × m^{-1} and 1.5 fr × m^{-1} occurring at 267–265 and 263–261 masl, respectively. In the unfractured dolostone interval 265–263 masl, the highest magnitude of the vertical component of hydraulic gradient occurs (–2.8 as shown in Fig. 10a). Here, lack of fractures in mechanically strong dolostone beds create the head loss instead of the presence of marl beds.

The VPV-01 borehole in Fig. 10b (entire Gasport Formation, Goat Island Formation, Eramosa and Guelph formations drilled) shows some similarities to GSMW2-09 (uppermost part of Gasport Formation, Goat Island Formation, Eramosa and Guelph formations drilled). The head loss occurs in multiple units with an overall head loss of 1.2 m and negligible head loss in the lower 32 m of the Gasport Formation (Fig. 10b). In all, 34% of the head loss occurs in the upper Gasport Formation (0.42 m), 29% in the Ancaster and Niagara Falls members of the Goat Island Formation (0.35 m), and 37% in the Vinemount Member (0.45 m) of the Eramosa Formation. The head loss varies in a thick interval (282–296 masl) that is characterized by a low fracturing frequency (≤1.0 fr × m^{-1}) with multiple 1-m-thick unfractured intervals and subvertical joints that are absent throughout the 14 m of poorly fractured dolostones. By contrast, the fracturing frequency is higher in the intervals of dolostones below (258–271 masl) and above (298–320 masl) the interval of occurrence of the head loss. High-angle joints are also more frequent in the upper and lower more highly fractured zones (Fig. 10b).

Another hydraulic scenario is observed in the SEN-07 borehole (Fig. 10c). In this borehole, the highest magnitude of vertical hydraulic gradient (–4.2) aligns with a thin (287–285 masl) marly dolostone interval that is poorly fractured (<2.0 fr × m^{-1}) with no high-angle joints. This zone is located between highly fractured intervals (>6.0 fr × m^{-1}). A single high-angle joint is present in both these relatively highly fractured intervals (289–287 and 285–283 masl; Fig. 10c). This sparsely fractured interval is part of the Vinemount Member where the gamma-ray counts are moderate (10–60 cps) but much higher than dolostone-dominated stratigraphic intervals below (gamma-ray counts < 20 cps). The vertical component of the hydraulic gradient is also relatively high (–1.8) for SEN-07 (Fig. 10c) in a 1.5-m interval (276–274 masl) that occurs in the uppermost portion of the Gasport Formation. This logged interval of dolostones is characterized by a fracture frequency of 0 with low gamma-ray counts (<20 cps).

A TD system installed at SEN-05 (Fig. 10d) shows a 10 m head loss across a 2.5-m interval (306–303.5 masl), resulting in a vertical component of a hydraulic gradient of –4.0. This stratigraphic interval has high natural gamma values (65 cps) and marly dolostones observed in the rock core. This interval occurs in the Ancaster Member of the Eramosa

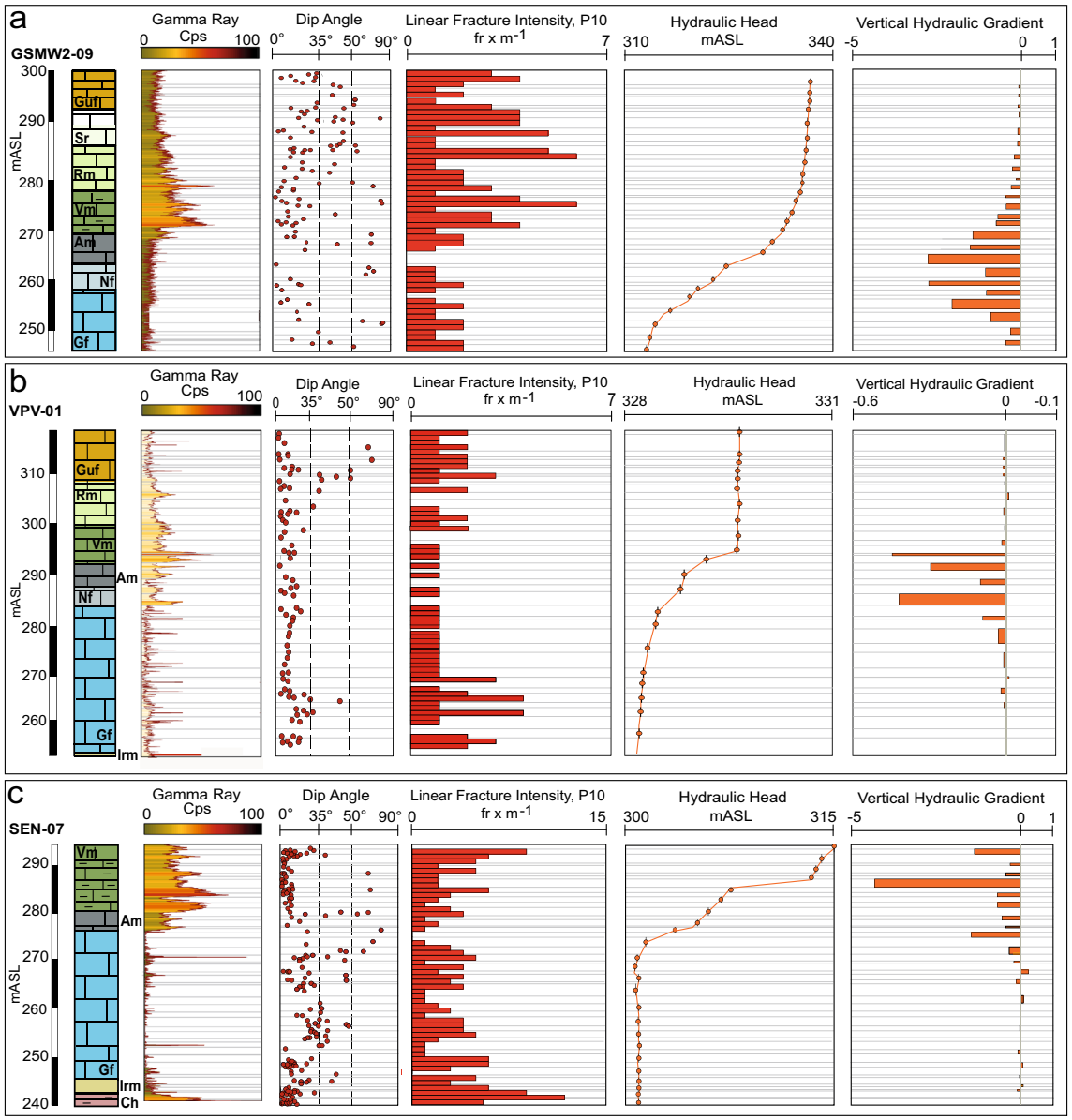

Fig. 10 Lithostratigraphic units, gamma-ray and hydraulic head profiles, and gradients showing the variety of stratigraphic occurrence and gamma-ray variations in Cps, fracture intensity, and head change/vertical gradient expressions in the Lockport Group at Guelph; the scales change in the logs to highlight variations of intensities. **a** GSMW2-09, **b** VPV-01, **c** SEN-7, **d** SEN-05, **e** Tier3-10, and **f** MW367-6 wells. Irondequoit, Rockway and Merritton formations (Irm), Cabot Head Formation (Ch), Gasport Formation (Gf), Niagara Falls (Nf) and Ancaster Member (Am) of the Goat Island Formation, Vinemount (Vm), Reformatory Quarry (Rm) and Stone Road (Sr) members of the Eramosa Formation, and Guelph Formation (Guf)

Formation, which is also poorly fractured (<1.0 fr × m^{-1}). The rock interval where the head loss occurs (306–303.5 masl) also shows a smaller interval where no high-angle and mechanically connective joints occur. Of note, three high-angle joints are present above (308–305.5 masl), and two below (306–301.5 masl), the interval where the head loss occurs.

This hydro-mechanical scenario fits the data collected in Tier3-10 using a Westbay™ MLS to determine the hydraulic head (Fig. 10e). Here, the majority of the head loss occurs in the thin Ancaster Member where high natural gamma values (55 cps) and marls are present 4.0 m below the bottom of the Eramosa Formation. Head loss (18.4 m) and a vertical component of gradient equal to –7.2 occurs in a 2.8-m thick, and poorly fractured (<1.0 fr × m^{-1}) interval (281.8–279 masl) with no high-angle joints. In the 2 m above (283.8–281.8 masl) and below

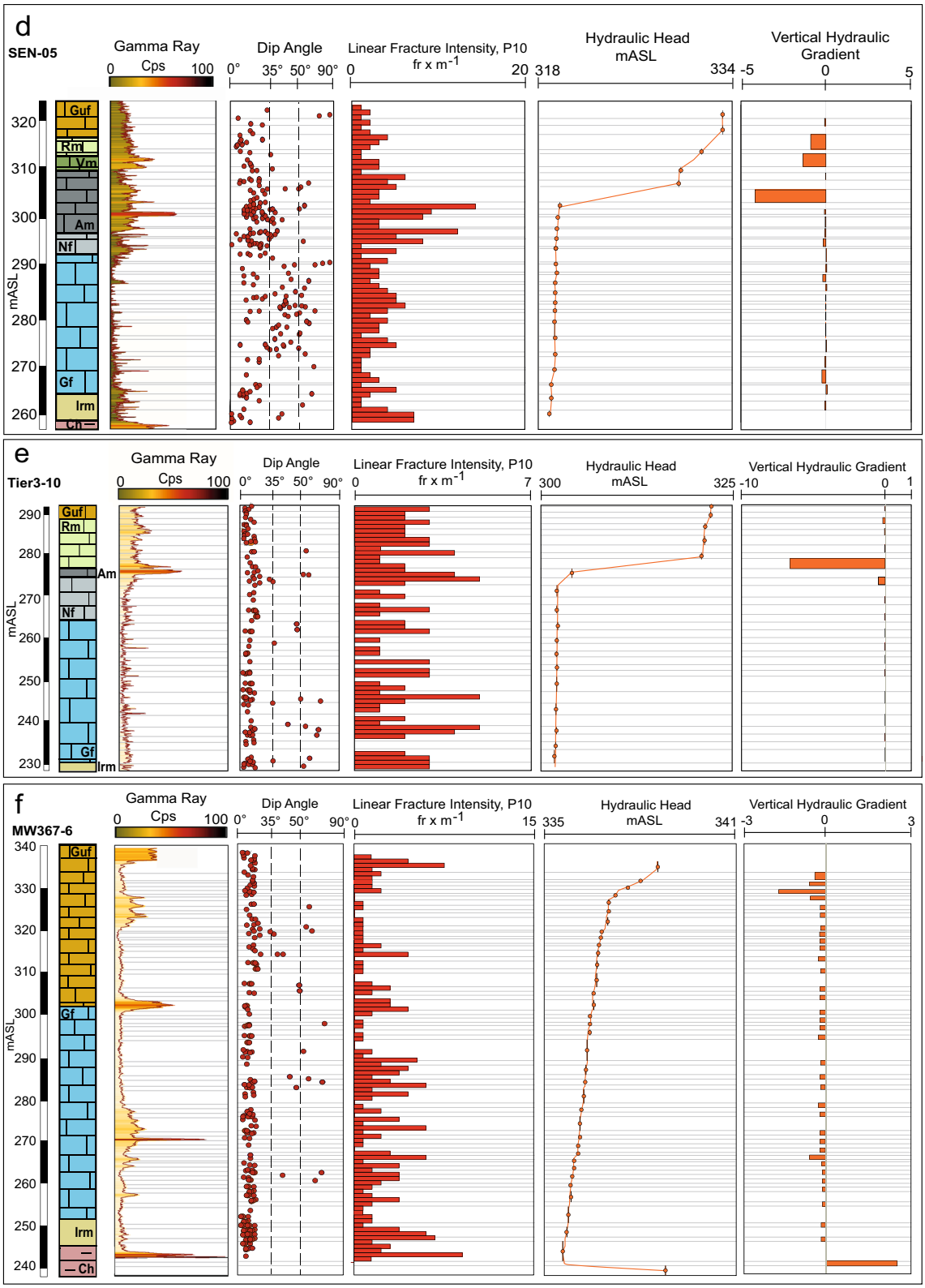

Fig. 10 (continued)

(279–277 masl) the head loss zone, high-angle joints occur with a frequency of 0.5 and 1.0 fr × m^{-1}, respectively.

In the northwestern sector of the city of Guelph (Fig. 1c), the Eramosa and the Goat Island formations are absent and head loss occurs in the upper Guelph Formation as seen in MW367-6 (Fig. 10f). Brunton and Brintnell (2020) have provided an alternative and revised interpretation of the lithostratigraphy at this location suggesting there may be a thick Goat Island Formation in this area between the Gasport and Guelph formations, contrasting their original interpretation and the authors of this study's subsequent interpretations that exclude the presence of this unit based on visual inspection of high-resolution rock core and geophysical logs. This variability in interpretation by the same individuals over time highlights the subjectivity and uncertainty in distinguishing these lithostratigraphic units and may be subject to re-evaluation and refinement in the future. A Westbay™ system with 45 ports installed in MW367-6 indicates a 0.90 m of head loss between 330–330.5 masl, showing a –1.8 vertical component of gradient (Fig. 10f). It is noteworthy that the minimal occurrence of head loss does not align with two major spikes in the natural gamma log: (1) in the middle of the Gasport Formation, and (2) at the erosional disconformity between the Guelph and Gasport formations. These very thin gamma spikes likely relate to remnants of the argillaceous material from the Eramosa and Goat Island formations that are absent in this location but occur nearby; or the concentration of clay minerals from a period of subaerial exposure and dissolution (Fig. 10f). Only minor and relatively uniform head loss is observed in the 58 m of Gasport Formation intercepted by MW367-6, possibly induced by fully penetrating water supply wells pumping in the Gasport Formation. The most transmissive interval in this borehole from straddle packer and FLUTe™ transmissivity profiling is in the lower one-quarter of the Gasport formation between 79.3 and 86.1 m below ground surface (mbgs; data not presented here). The Gasport Formation is highly transmissive and has a bulk horizontal hydraulic conductivity 1–3 times higher than the Guelph Formation according to straddle and pumping test data (Table 1).

Overall, the position of the head loss observed in these boreholes is variable—SEN-07 has 11.67 m, SEN-05 has 10 m (Fig. 10d), VPV-01 has 1.2 m (Fig. 10b), and Tier3-10 has 18.4 m (Fig. 10e) of head loss primarily within the Goat Island and Eramosa formations. MW367-6 has 3 m of head loss occurring largely in the upper Guelph Formation (Fig. 10f). The vertical hydraulic gradient varies significantly in the uppermost Gasport Formation in GSMW2-09 (Fig. 10a). In this borehole, only data from the uppermost 12 m of Gasport Formation exists.

Discussion

New findings

Hydrologic units and aquitards are often inferred, depending on lithostratigraphic units at the scale of either members or geological formations in carbonate successions (e.g., Moya et al. 2014; Smerdon and Gardner 2022). In this study, lithostratigraphic units were found to not be predictive of aquitard position or thickness in a Silurian dolostone succession based on a large dataset of rock discontinuities (Tables 3, 4 and 5; Figs. 6, 7, 8 and 9, and Figs. S2 and S3 of the ESM), and high-resolution head data in vertical profile at two dozen locations (Table 6; Fig. 10 and Fig. S4 of the ESM). The combination of hydraulic head profiles and rock discontinuity data from vertical and inclined boreholes and scanlines at outcrops shows the aquitard units to appear more heterogeneous than expected, as depicted in the conventional conceptual models in Figs. 11 and 12. According to the high-resolution multilevel hydraulic head monitoring systems, head loss relating to lower vertical hydraulic conductivity was measured in all of the observed lilthostratigraphic units of the Lockport Group (Fig. 11).Informed by hydraulic head profiles from 24 locations, some degree of consistency exists regarding the hydraulic head occurrence in the Lockport Group across the city of Guelph, as shown in Table 6. Inflections of the hydraulic head do not occur in the lower and intermediate portions of the Gasport Formation. Head inflections in the Gasport Formation, if present, appear to occur exclusively in the upper 8 m (Table 6), below which, the formation appears to be hydraulically well connected vertically. The upper Gasport head inflections could be related to the gradual lithological transition to the Goat Island Formation that occurs locally (Brunton and Brintnell 2020). Overall, the Gasport Formation is a productive aquifer unit that (1) is thickly bedded (Table 4); (2) has relatively long joints that are 0.1–3 m in height as shown by 192 measurements collected in an outcrop located 7.5 km northeast of the city of Guelph (Kunert and Coniglio 2002; Cole et al. 2009); and (3) has particularly high bulk hydraulic conductivities (Table 1). These high values of hydraulic conductivity at the packer and pumping test scales are 1–3 orders of magnitude higher than those in the other geological units (Guelph, Eramosa, and Goat Island formations) due to either connectivity of joints (contributing to increased K_v), and enhanced apertures of laterally extensive bedding plane discontinuities (contributing to high K_h) enlarged by groundwater dissolution as shown in the core and ATV logs (Skinner 2019; Munn et al. 2020).

Comparisons of the ATV log fracture datasets and the high-resolution hydraulic head profiles from the same boreholes show an association of low fracture frequency

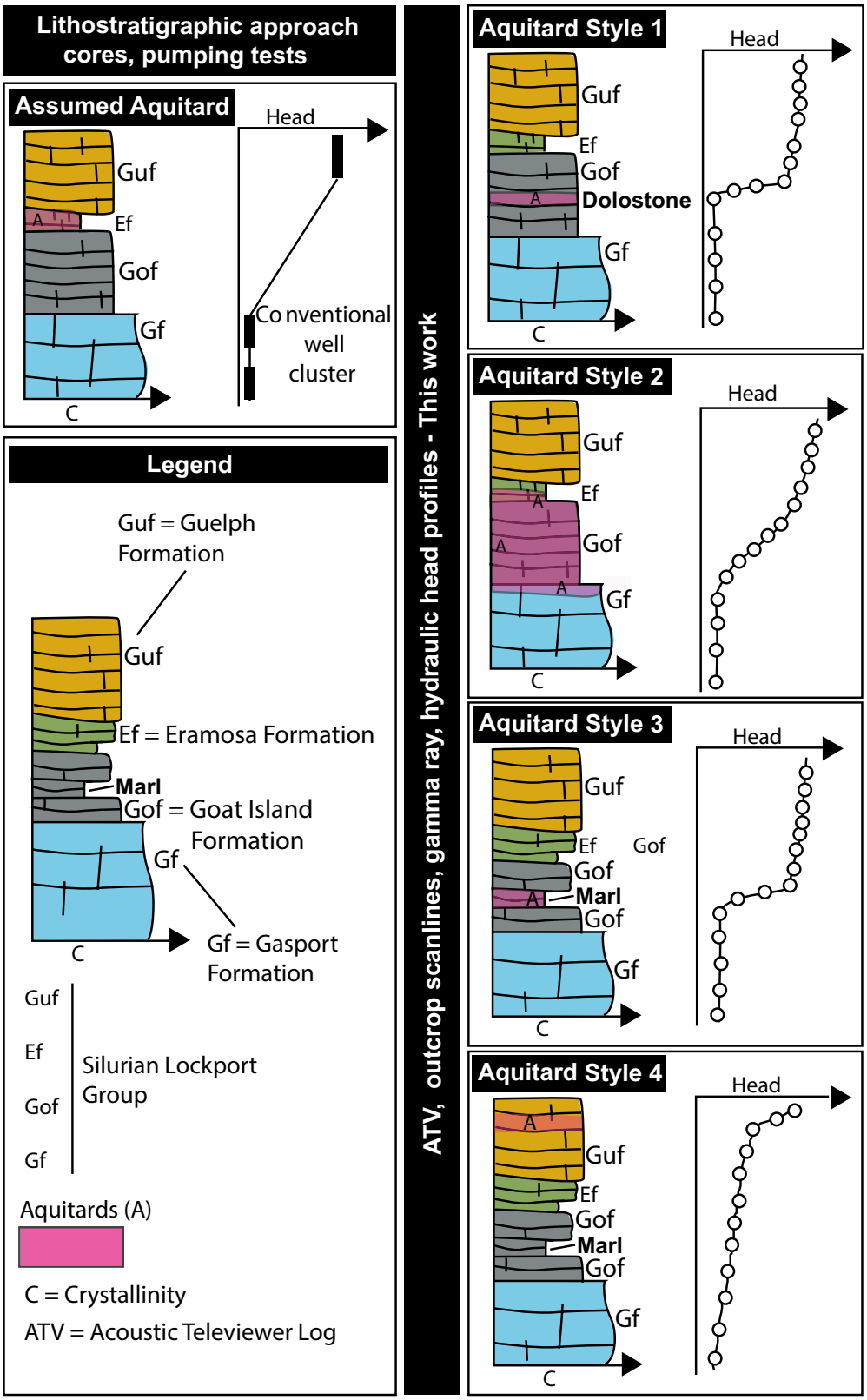

Fig. 11 Conceptual scheme of the system of aquitards and hydraulic head occurrence that compares the traditional approach with conventional well clusters, cores and pumping tests, and Morwick G[360] Groundwater Research Institute (MG360) hydro-geophysical investigation based on ATV, outcrop scanlines, gamma-ray and hydraulic head profiles. The approach presented here allows four different styles of head loss occurrence to be detected that are illustrated in the conceptual scheme

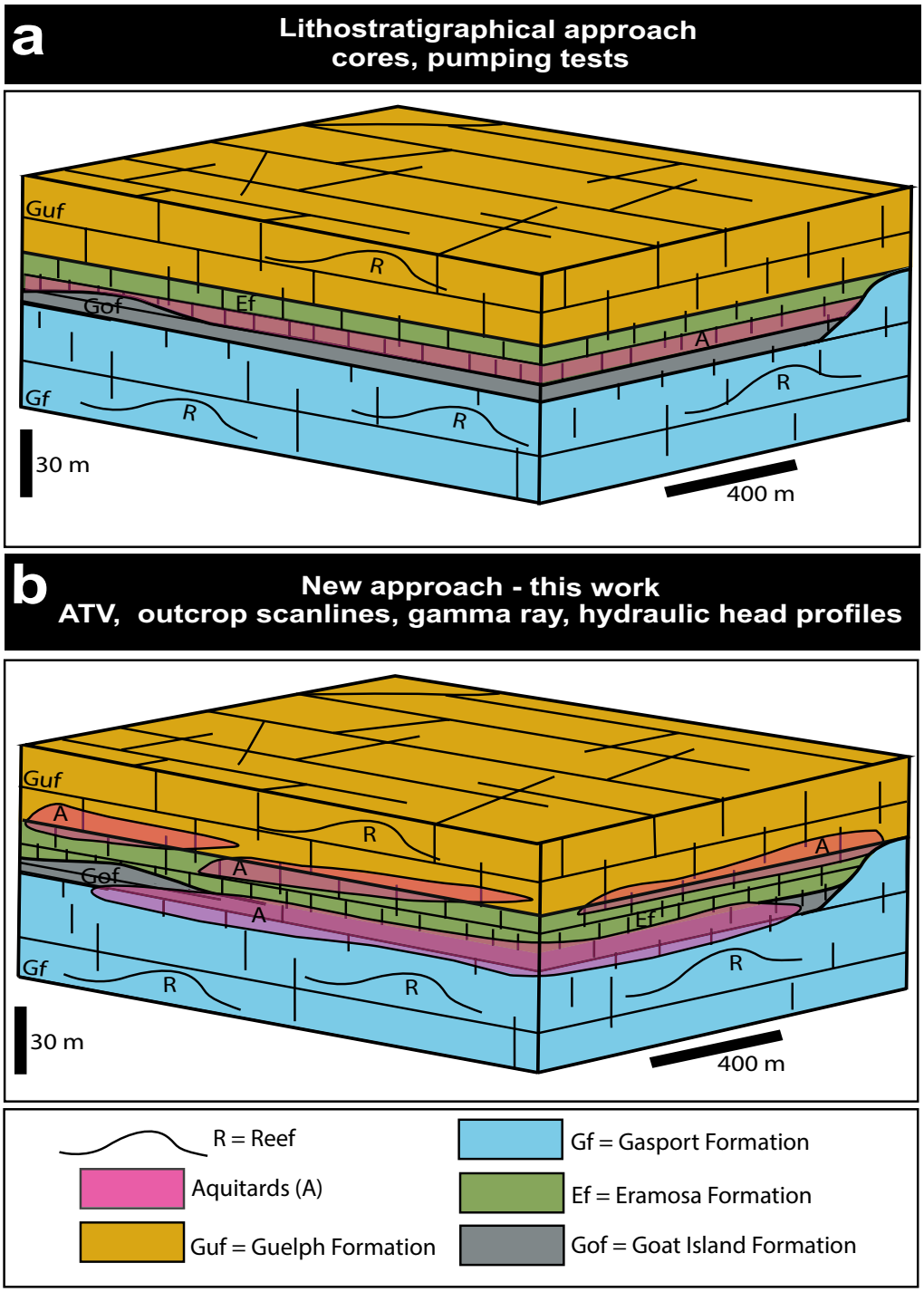

Fig. 12 3D conceptual scheme of the system of aquitards; **a** traditional approach with cores and pumping tests, and styles at the study site, and **b** (MG360) hydro-geophysical investigation based on ATV, outcrop scanlines, gamma-ray and hydraulic head profiles

of the high-angle joints within the occurrence of large inflections in hydraulic head, showing changes in the vertical hydraulic gradient magnitude in the Eramosa and Goat Island formations. Here, important inflections of the hydraulic head occur where thin 2–2.5-m rock intervals show no high-angle joints. These conditions exist in three of the six boreholes (SEN-07 in Fig. 10c, SEN-05 in Fig. 10d and Tier3-10 in Fig. 10e). These mechanical interfaces (changes in cumulative fracture frequency with depth) that coincide with inflections in hydraulic head can occur in either (1) thin marl beds with high natural gamma values; or (2) thin (2–2.5 m) finely grained

dolostones with bed parallel laminations (see sedimentological details for the Ancaster Member in Brunton and Brintnell 2020). Head loss occurs most frequently in the Ancaster Member of the Goat Island Formation according to the data summary in Table 6. This finding does not imply that the occurrence of head loss across marl beds of the Eramosa Formation are scarce. Such head inflections have been detected in most boreholes where the Vinemount Member is present, but the presence or thickness of this unit and the nature of the head loss are not consistent across the city of Guelph. The marls in outcrops are highly variable and show either the characteristics of a preferential pathway (abundance of high-angle joints that crosscut beds) or characteristics that could represent a barrier to flow (shallower joint dip angles, joint terminations at bedding plane discontinuities, and lower joint heights than in dolostones). The marl beds, which are often thinly layered (arithmetic average of bed thickness: 5 cm from outcrop scanlines), can impede the vertical propagation of the high-angle joints (Fig. 4a,c), and are characterized by lower dip angles in outcrops as shown by the quarry walls (Fig. 4b) collected at the Reformatory Quarry in Guelph (Fig. 8b). This pattern has also been noticed by structural geologists in the Silurian carbonates in northeastern Wisconsin (Underwood et al. 2003). The marl beds are therefore capable of reducing vertical hydraulic conductivities, which results in inflections of the hydraulic head profiles in some cases (Fig. 10e). However, 72 and 68% of the joints internal to the mechanical unit either contact (termination types 2, 3, and 8) or crosscut (termination types 4, 5, 6, 7, and 9) the bedding planes in marly and dolostone beds, respectively (Fig. 9b). According to these percentages, the marls do not represent perfect barriers for vertical groundwater flow, which is consistent with the observed minimal head loss across marl rich layers as denoted by the many small natural gamma spikes in the boreholes presented in Fig. 10.

The interplays between the three mechanical factors are the height of the joints, fracture frequency of the joints, and types of joint termination that are difficult to observe in borehole logs yet readily observed at the quarry walls, and that are associated with four styles of hydraulic head inflections (Fig. 11). Aquitard style 1 shows head loss occurring over thin (1–3 m) dolostone layers characterized by no high-angle joints (e.g., Fig. 10b). It is noteworthy that style 1 can occur in all the lithostratigraphic units, yet the Ancaster Member is more prone to this style of hydraulic head loss due to the low frequency of high-angle joints across the study area (Table 4).

Aquitard style 2 shows head loss occurring over thicker intervals (≤18 m) also depicted in Fig. 11. In this case, multiple poorly fractured intervals with no or few high-angle joints can occur within a thicker sequence. The third aquitard style (style 3) occurs when head loss is localized across thin (0.1–3 m) marly layers. Examination of the statistics on joint terminations in Fig. 9b reveals that vertical joints, although very short, crosscut the marls slightly more frequently than the dolostone layers. Although these marls are characterized by small fractures, they can fail at being vertical barriers (style 3), and other styles (1 and 2, Fig. 11) of vertical reduction of hydraulic conductivities can occur in dolostone beds. Of note, styles 1 and 2 show two common features and the head loss can occur across thin intervals of rocks within a lithostratigraphic unit. A fourth style (style 4) occurs in the absence of a thick marly interval in the uppermost part of the Silurian dolostone sequence. In this case, the head loss occurs in a carbonate interval, but not in the lower and intermediate portions of the stratigraphic sequence that are characterized by massive beds and very long joints. Overall, the four styles illustrated in Fig. 11 advance the previous conceptualization of this Silurian sequence where an aquitard was systematically assigned to a 5–15-m-thick marly geological member. The fourth style incorporates the observation that the principal aquitard can occur at different sublithostratigraphic levels and is not necessarily associated with observable fracture or lithological changes, and can be much thinner than 5–15 m (Fig. 11).

New research scenarios

The bulk hydraulic conductivity in fractured rock aquifers is strongly influenced by fracture connectivity; therefore, zones of lower vertical hydraulic conductivity are expected where fracture connections are limited due to terminations or closure (Aydin 2000). This study is novel in that it shows the connection between the fracture characteristics and the style of hydraulic head loss observed at multiple locations in a Silurian dolostone sequence. In addition, this study introduces a new scanline method for use in outcrop mapping for classifying the type of joint termination or characteristics (Fig. 9a). These fracture termination datasets, while not fully predictive of aquitard properties on their own, can be identified with high-resolution head profiles to provide additional insights into the mechanism of head loss within the dolostone sequence. This approach has identified likely causes for nonsystematic occurrences of head loss (and lack of head loss) in the full thickness of the marl-rich Vinemount Member of the Eramosa Formation, in contrast with the traditional assumption that the presence and entire thickness of this member can be assigned aquitard properties (Figs. 11 and 12a). Head loss, as well as the reduced vertical hydraulic conductivity associated with aquitards, has been observed within all the lithostratigraphic units of the Lockport Group, and therefore the position of these low K_v units can be challenging to predict from geologic data alone.

The aquitard units throughout the multilayered Silurian dolostone sequence seem to be characterized by multiple patches of limited lateral extent and variable thickness providing a conceptual picture very different from the traditional view either vertically (Fig. 11) or laterally (Fig. 12b). The minimum lateral extension of these patches has been recently constrained by Skinner (2019) to 800 m (Fig. 2a) using multiple MLSs shown along the cross-sections. However, cross-referencing the information from geological cross-sections at larger scales with the hydraulic data in Table 6 makes it difficult to laterally constrain the patches using hydraulic head profiles for distances over 3,000 m (Fig. 2b,c). The lateral extension of the patches is less than 3,000 m in the geological cross section in Fig. 2b where the head loss moving laterally occurs at different depths and in different lithostratigraphic units. Therefore, this study reinforces the need for further detailed hydraulic head profiles to identify the position, lateral continuity and thickness of aquitard units in fractured carbonate aquifers to provide reliable definition of the 3D groundwater flow system influencing groundwater flow trajectories linking recharge and discharge points (i.e. capture zones) and residence times.

This research combines high-resolution hydraulic head profiles most notably derived from Westbay™ multilevel monitoring systems and strings of transducers temporarily deployed behind liners (i.e. TD systems) that provided dozens of depth-discrete hydraulic head profile locations across the Silurian dolostone unit thickness with fracture data from outcrop and high-resolution logs from vertical and inclined boreholes. The majority of these techniques (analysis of fractures in outcropping reservoir analogues, geophysics in vertical and inclined wells, and Westbay MLS or TD systems) have been used in the shallow sedimentary bedrock aquifers of Wisconsin and Minnesota (Runkel et al. 2018) and Ontario (this research) in areas characterized by subhorizontal beds in continental platforms. Similar methods have also been used, but not analysed together, across other geosciences disciplines such as the determination of cap rock suitability in CO_2 storage in deep saline aquifers in tectonically deformed areas (Aydin 2000; Proietti et al. 2023). The suitability of rock to be either an aquitard or a cap-rock depends on the capacity of the rock to reduce the vertical hydraulic conductivity associated with joint terminations. Such joint terminations are difficult to use alone in a predictive manner, but when combined with high-resolution hydraulic head profiles, they can potentially be used to improve the basis for aquitard delineation with confidence in other fractured rock systems.

The joint termination used in this work has been acquired by performing scanline surveys in the field on quarry faces. This parameter can also be determined using unmanned aerial vehicles as well as the LiDAR tablets that are currently spreading widely within the geo-engineering community (e.g., Allmendinger et al. 2017; Medici et al. 2023b). Overall, the proposed approach demonstrates the combining of fracture analysis, incorporating the type of joint termination with high-resolution hydraulic head profiles, to be feasible and promising for improved flow system characterization, useful to many geoscience fields such as contaminant hydrology, natural resources extraction (i.e. water supply hydrogeology, mining, oil/gas) and waste isolation such as the currently and emerging topic of CO_2 storage.

Conclusion

This paper describes the combination of high-resolution hydraulic head profiles with rock discontinuity statistics derived from vertical and inclined boreholes and outcrops to determine the factors that affect the occurrence of head loss and its degree of spatial predictability in the Silurian Dolostone below the city of Guelph, ON. The presented research can be summarized in four key findings, all unknown before applying this multimethod field approach:

1. High-angle joints crosscut dolostone and marl beds in 5.1 and 27.9% of the measurements, respectively. An analysis of the rock discontinuities reveals that the marls are characterized by shorter joints, and shallower dip angles relative to the dolostones in outcrop. However, high-angle joints more frequently crosscut the bedding plane fractures in marls relative to dolostones and, therefore, do not appear to represent consistent barriers (lower K_v units) for reducing vertical groundwater flow.
2. Three mechanical factors appear to play a role in the aquitard properties in a carbonate succession containing interbedded marls: (1) fracture frequency of the high-angle joints; (2) joint height; and (3) the type of termination of high-angle joints with bedding plane fractures (i.e. connectivity). Inflections of hydraulic head occur most commonly in substratigraphic intervals with low fracture frequency. The inflections do not occur in thickly bedded or massive intervals containing long joints. In such intervals, the head is more uniform (negligible vertical components of gradient) across thicknesses greater than 20 m such as within the lower Gasport Formation.
3. Four styles of head-loss are identified in the Silurian fractured carbonates in the southern Ontario study. Head loss occurs in relatively thin (1–3 m) dolostone layers with a low frequency of high-angle joints ($<1.0\ n^0 \times m^{-1}$ of fracture frequency; style 1). These unfractured dolostones can occur multiple times in the stratigraphic sequence in layers $\leq$18 m thick; here the head loss occurs over a broader interval, representing style 2. The head loss occurs in a few cases in thin (0.1–3 m thick)

marly and poorly fractured layers embedded in relatively thick and heavily fractured intervals of dolostone beds (style 3). A fourth style occurs in the absence of a thick marly interval in the uppermost part of the Silurian dolostone sequence. In style 4, the head loss occurs in a carbonate interval, but not in the lower and intermediate portions of the stratigraphic sequence characterized by massive beds and very long joints.

4. This data-intensive investigation reveals that the head loss can occur within any of the lithostatigraphic units of the Lockport Group, except within the lower and intermediate part of the Gasport Formation, which is hydraulically well connected in all cases. The dolostone and marl intervals containing either low fracture intensity or unconnected joints that do not crosscut the bedding planes are abundant, laterally discontinuous and vertically stacked. This hydro-mechanical pattern makes the effective aquifer/aquitard sequence significantly more complex than inferring hydraulic properties based on lithostratigraphy alone, and reinforces the value of high-resolution head profiles for delineating hydrogeological units informing 3D groundwater flow systems.

Overall, the statistics calculated for the geometry, frequency and termination of rock discontinuities are the largest reported in the hydrological literature among fractured sedimentary rocks. The combination of high-spatial-resolution techniques (outcrop scanlines, gamma-ray and ATV logs from vertical and inclined boreholes combined with hydraulic head profiles) are used both in the fields of contaminant hydrogeology and geological carbon storage in shallow and deep aquifers, respectively. Therefore, these findings are relevant for determining aquitard or cap-rock properties in other heterogeneous carbonate sedimentary sequences.

Supplementary Information The online version contains supplementary material available at https://doi.org/10.1007/s10040-024-02824-9.

Acknowledgements The data used in this study was collected by Morwick G360 graduate students and staff as part of Dr. Parker's research program from 2006 to 2020. The manuscript benefitted from constructive discussions regarding the interpretation of field data sets with Morwick G360 staff scientists including Dr. Jonathan Kennel, Dr. Peeter Pehme, Chrystyn Skinner and Marina Nunes. Kely Alejo, Emily Cline and Andrew Stockford supported outcrop mapping in the field, and Laura Weaver supported data quality assurance and retrieval. The manuscript benefitted from constructive comments by Dave Belanger (hydrogeologist with the City of Guelph) and journal reviewers: Tony Runkel (Minnesota Geological Survey), the editor Maria-Theresia Schafmeister (University of Greifswald), the associate editor Peter Kang (University of Minnesota) and one anonymous reviewer.

Funding Open access funding provided by Università degli Studi di Roma La Sapienza within the CRUI-CARE Agreement. The authors acknowledge the Natural Sciences Engineering Research Council of Canada Contract Research and Development Grant NSERC CRDPJ 525892-18 to Drs. Beth Parker, Arnaud, Levison and Gharabaghi, with matching funds from the city of Guelph and Blue Triton Brand and NSERC Alliance Grant ALLRP 568604-21 to Drs. Jonathan Munn, Beth Parker, and Jana Levison, for supporting the Postdoctoral Fellowship to the lead author. Data collection was supported by previous grants led by Dr. Beth Parker, specifically NSERC Grant IRCPJ grants (363783-06, 363783-11, 363783-18) since 2007; NSERC Grant CRDPJ (489241-15) and the Ontario Research Fund Grant (RE-03-061).

Declarations

Conflict of interest On behalf of all co-authors, the corresponding authors state that there is no conflict of interest.

References

Agbotui PY, West LJ, Bottrell SH (2020) Characterisation of fractured carbonate aquifers using ambient borehole dilution tests. J Hydrol 589:125191

Allmendinger RW, Cardozo N, Fisher D (2012) Structural geology algorithms: vectors and tensors. Cambridge University Press, Cambridge

Allmendinger RW, Siron CR, Scott CP (2017) Structural data collection with mobile devices: accuracy, redundancy, and best practices. J Struct Geol 102:98–112

Arnaud E, McGill M, Trapp A, Smith JE (2018) Subsurface heterogeneity in the geological and hydraulic properties of the hummocky Paris Moraine, Guelph, Ontario. Can J Earth Sci 55(7):768–785

Aydin A (2000) Fractures, faults, and hydrocarbon entrapment, migration and flow. Marin Petrol Geol 17(7):797–814

Berkowitz B (2002) Characterizing flow and transport in fractured geological media: a review. Adv Water Resour 25:861–884

Brett CE, Goodman WM, LoDuca ST (1990) Sequences, cycles, and basin dynamics in the Silurian of the Appalachian Foreland Basin. Sediment Geol 69:191–244

Brunton FR, Brintnell C (2020) Early Silurian sequence stratigraphy and geological controls on karstic bedrock groundwater-flow zones, Niagara Escarpment region and the subsurface of southwestern Ontario. Groundwater Resources Study 13, Ontario Geological Survey, Sudbury, ON

Capes CC, Steelman CM, Parker BL (2018) Hydrologic interpretation of seasonally dynamic ambient temperature profiles in sealed bedrock boreholes. J Hydrol 567:133–148

Carannante G, Esteban M, Milliman JD, Simone L (1988) Carbonate lithofacies as paleolatitude indicators: problems and limitations. Sediment Geol 60(1–4):333–346

Carter JM (2002) USGS definition of terms, atlas of water resources in the black hills area. Sioux Falls, South Dakota

Cherry JA, Parker BL, Keller C (2007) A new depth-discrete multilevel monitoring approach for fractured rock. Ground Water Monit Remediat 27:57–70

Chow SJ, Croll HC, Ojeda N, Klamerus J, Capelle R, Oppenheimer J, Jacangelo JG, Schwab KJ, Prasse C (2022) Comparative investigation of PFAS adsorption onto activated carbon and anion exchange resins during long-term operation of a pilot treatment plant. Water Res 226:119198

Cole J, Coniglio M, Gautrey S (2009) The role of buried bedrock valleys on the development of karstic aquifers in flat-lying carbonate bedrock: insights from Guelph, Ontario, Canada. Hydrogeol J 17:1411–1425

Ely DM, Bachmann MP, Vaccaro JJ (2011) Numerical simulation of groundwater flow for the Yakima River basin aquifer system, Washington. Report 2011–5155, US Geological Survey, Reston, VA

Eyles N, Arnaud E, Scheidegger AE, Eyles CH (1997) Bedrock jointing and geomorphology in southwestern Ontario, Canada: an example of tectonic predesign. Geomorphology 19:17–34

Fernandes J (2017) Nature and extent of toluene contamination in a shallow dolostone aquifer using high resolution methods for assessing natural and anthropogenic influences. MSc Thesis, University of Guelph, Guelph, ON, Canada

Formenti S, Peace A, Eyles C, Lee R, Waldron JW (2023) Fractures in the Niagara Escarpment in Ontario, Canada: distribution, connectivity, and geohazard implications. Geol Mag 159(11–12):1936–1951

Golder (2011) City of Guelph southwest quadrant water supply class environmental assessment. Report no. 07-1112-0059, Golder, Mississauga, ON, Canada

Hartmann A, Goldscheider N, Wagener T, Lange J, Weiler M (2014) Karst water resources in a changing world: review of hydrological modeling approaches. Rev Geophys 52:218–242

Howroyd M, Novakowski KS (2021a) Interpretation of a network-scale tracer experiment in fractured rock conducted using open wells. J Contam Hydrol 243:103907

Howroyd M, Novakowski KS (2021b) The use of scaling parameters and the impact of non-uniqueness in the simulation of a large-scale solute transport experiment conducted in discrete fractures. J Contam Hydrol 243:103890

Howroyd M, Novakowski KS (2022) Allocating transmissivities from constant head tests for the development of DFN models. Can Geotech J 59:87–100

Hitchmough AM, Riley MS, Herbert AW, Tellam JH (2007) Estimating the hydraulic properties of the fracture network in a sandstone aquifer. J Contam Hydrol 93:38–57

Huh JM, Biggs LI, Gill D (1977) Depositional environment of Pinnacle Reffs, Niagara and Salina groups, Northern Shelf, Michigan Basin. In: Reefs and evaporites: concepts and depositional models. AAPG, Tulsa, OK, pp 1–21

Johnson K (2020) High resolution dynamic pore pressure monitoring to determine hydraulic parameters in a multi-layered bedrock system for improved aquifer vulnerability assessment and monitoring. MSc Thesis, University of Guelph, Guelph, ON, Canada

Kamilo UCGL (2012) A nitrate impacted groundwater study in the overburden and Silurian dolostone aquifer in an agricultural area within the Torrance Creek Watershed, Guelph, Ontario. MSc Thesis, University of Waterloo, Waterloo, ON, Canada

Kosakowski G, Berkowitz B (1999) Flow pattern variability in natural fracture intersections. Geophys Res Lett 26:1765–1768

Kunert M, Coniglio M (2002) Origin of vertical shafts in bedrock along the Eramosa River valley near Guelph, southern Ontario. Can J Earth Sci 39(1):43–52

Leite K (2015) A nitrate impacted groundwater study in the overburden and Silurian bedrock aquifer in an agricultural area within the Torrance Creek Watershed Guelph: Ontario-Canada. MSc Thesis, University of Guelph, Guelph, ON, Canada

Lemieux JM, Therrien R, Kirkwood D (2006) Small scale study of groundwater flow in a fractured carbonate-rock aquifer at the St-Eustache quarry, Québec, Canada. Hydrogeol J 14:603–612

Lorenzi V, Banzato F, Barberio MD, Goeppert N, Goldscheider N, Gori F, Lacchini A, Menetta M, Medici G, Rusi S, Petitta M (2024) Tracking flowpaths in a complex karst system through tracer test and hydrogeochemical monitoring: implications for groundwater protection (Gran Sasso, Italy). Heliyon 10(2):e24663. https://doi.org/10.1016/j.heliyon.2024.e24663

Maldaner CH, Munn JD, Coleman TI, Molson JW, Parker BL (2019) Groundwater flow quantification in fractured rock boreholes using active distributed temperature sensing under natural gradient conditions. Water Resour Res 55(4):3285–3306

Maldaner CH, Quinn PM, Cherry JA, Parker BL (2018) Improving estimates of groundwater velocity in a fractured rock borehole using hydraulic and tracer dilution methods. J Contam Hydrol 214:75–86

Mancini A, Della Porta G, Swennen R, Capezzuoli E (2021) 3D reconstruction of the Lapis Tiburtinus (Tivoli, Central Italy): the control of climatic and sea-level changes on travertine deposition. Basin Res 33(5):2605–2635

Maurice LD, Atkinson TC, Barker JA, Williams AT, Gallagher AJ (2012) The nature and distribution of flowing features in a weakly karstified porous limestone aquifer. J Hydrol 438:3–15

Medici G, West LJ (2023) Reply to discussion on 'Review of groundwater flow and contaminant transport modelling approaches for the Sherwood Sandstone aquifer, UK: insights from analogous successions worldwide' by Medici and West (QJEGH, 55, qjegh2021-176). Q J Eng Geol Hydrogeol 56(1):qjegh2022-097. https://doi.org/10.1144/qjegh2022-097

Medici G, West LJ, Banwart SA (2019) Groundwater flow velocities in a fractured carbonate aquifer-type: implications for contaminant transport. J Contam Hydrol 222:1–16

Medici G, Lorenzi V, Sbarbati C, Manetta M, Petitta M (2023a) Structural classification, discharge statistics, and recession analysis from the springs of the Gran Sasso (Italy) carbonate aquifer: comparison with selected analogues worldwide. Sustainability 15(13):10125

Medici G, Ling F, Shang J (2023b) Review of discrete fracture network characterization for geothermal energy extraction. Front Earth Sci 11:1328397

Meyer JR, Parker BL, Cherry JA (2008) Detailed hydraulic head profiles as essential data for defining hydrogeologic units in layered fractured sedimentary rock. Environ Geol 56:27–44

Meyer JR, Parker BL, Cherry JA (2014) Characteristics of high resolution hydraulic head profiles and vertical gradients in fractured sedimentary rocks. J Hydrol 517:493–507

Meyer JR, Parker BL, Arnaud E, Runkel AC (2016) Combining high resolution vertical gradients and sequence stratigraphy to delineate hydrogeologic units for a contaminated sedimentary rock aquifer system. J Hydrol 534:505–523

Meyer JR, Parker BL, Abbey DG, Shikaze, SG, Weaver L, Merritt G, Runkel AC (2023) Rock core VOC profiles diagnostic of aquitard occurrence and integrity in a multi-layered sedimentary rock aquifer flow system. J Hydrol 626. https://doi.org/10.1016/j.jhydrol.2023.130347

Moore JP, Walsh JJ (2021) Quantitative analysis of Cenozoic faults and fractures and their impact on groundwater flow in the bedrock aquifers of Ireland. Hydrogeol J 29:2613–2632

Moya CE, Raiber M, Cox ME (2014) Three-dimensional geological modelling of the Galilee and central Eromanga basins, Australia: new insights into aquifer/aquitard geometry and potential influence of faults on inter-connectivity. J Hydrol Reg Stud 2:119–139

Munn JD (2012) High-resolution discrete fracture network characterization using inclined coreholes in a Silurian dolostone aquifer in Guelph, Ontario. MSc, University of Guelph, Guelph, ON, Canada

Munn JD, Maldaner CH, Coleman TI, Parker BL (2020) Measuring fracture flow changes in a bedrock aquifer due to open hole and pumped conditions using active distributed temperature sensing. Water Resour Res 56(10). https://doi.org/10.1029/2020WR027229

Neymeyer A, Williams RT, Younger PL (2007) Migration of polluted mine water in a public supply aquifer. Q J Eng Geol Hydrogeol 40:75–84

Nunes MA, Aravena R, Parker BL (2021) Geochemical and isotopic evidence for pumping-induced impacts to bedrock groundwater quality in the City of Guelph, Canada. Sci Total Environ 800:149359

Odling NE, Gillespie P, Bourgine B, Castaing C, Chiles JP, Christensen NP, Fillion E, Genter A, Olsen C, Thrane L, Trice R (1999) Variations in fracture system geometry and their implications for fluid flow in fractures hydrocarbon reservoirs. Petrol Geosci 5:373–384

Odling NE, West LJ, Hartmann S, Kilpatrick A (2013) Fractional flow in fractured chalk: a flow and tracer test revisited. J Contam Hydrol 147:96–111

Parker BL, Cherry J, Swanson BJ (2006) A multilevel system for high-resolution monitoring in rotosonic boreholes. Ground Water Monit Rem 26(4):56–73

Parker BL, Bairos K, Maldaner CH, Chapman SW, Turner CM, Burns LS, Plett J, Carter R, Cherry JA (2019) Metolachlor dense non-aqueous phase liquid source conditions and plume attenuation in a dolostone water supply aquifer. Geol Soc Spec Publ 479:207–236

Pehme PE, Parker BL, Chapman SW, Cherry JA (2014) Temporary sensor deployments: a method for improved insight into hydraulic variations and design of permanent multilevel installations. Proceedings of International Discrete Fracture Network Engineering Conference, Vancouver, Canada, October 2014, 239 pp

Perrin J, Parker BL, Cherry JA (2011) Assessing the flow regime in a contaminated fractured and karstic dolostone aquifer supplying municipal water. J Hydrol 400:396–410

Priebe EH, Brunton FR, Rudolph DL, Neville CJ (2019) Geologic controls on hydraulic conductivity in a karst-influenced carbonate bedrock groundwater system in southern Ontario, Canada. Hydrogeol J 27:1291–1308

Priebe EH, Frape SK, Jackson RE, Rudolph DL, Brunton FR (2021) Tracing recharge and groundwater evolution in a glaciated, regional-scale carbonate bedrock aquifer system, southern Ontario, Canada. J Appl Geochem 124:104794

Proietti G, Conti A, Beaubien SE, Bigi S (2023) Screening, classification, capacity estimation and reservoir modelling of potential CO2 geological storage sites in the NW Adriatic Sea, Italy. Int J Greenh Gas Control 126:103882

Quinn PM, Cherry JA, Parker BL (2011) Quantification of non-Darcian flow observed during packer testing in fractured sedimentary rock. Water Resour Res 47(9). https://doi.org/10.1029/2010WR009681

Rivett MO, Buss SR, Morgan P, Smith JW, Bemment CD (2008) Nitrate attenuation in groundwater: a review of biogeochemical controlling processes. Water Res Res 42:4215–4232

Runkel AC, Robert GT, Julia RS, Andrew JR, Meyer JR, Parker BL, Green JA, Barry JD, Jones PM (2018) A multidisciplinary-based conceptual model of a fractured sedimentary bedrock aquitard: improved prediction of aquitard integrity. Hydrogeol J 26(7):2133–2159

Rustichelli A, Di Celma C, Tondi E, Bianucci G (2016) Deformation within the Pisco basin sedimentary record (southern Peru): strata-bound orthogonal vein sets and their impact on fault development. J South Am Earth Sci 65:79–100

Salek M, Levison J, Parker B, Gharabaghi B (2018) CAD-DRASTIC: chloride application density combined with DRASTIC for assessing groundwater vulnerability to road salt application. Hydrogeol J 26(7):2379–2393

Skinner C (2019) High-resolution hydrogeological characterization of a fractured dolostone municipal supply aquifer to create a refined 3-D conceptual site model with hydrogeologic units. MSc Thesis, University of Guelph, Guelph, ON, Canada

Smerdon BD, Gardner WP (2022) Characterizing groundwater flow paths in an undeveloped region through synoptic river sampling for environmental tracers. Hydrol Proces 36:14464

Stantec (2009) Guelph south groundwater supply investigation: final report City of Guelph. Report 160900499, Stantec, Guelph, ON, Canada

Steelman CM, Meyer JR, Parker BL (2017) Multidimensional investigation of bedrock heterogeneity/unconformities at a DNAPL-impacted site. Groundwater 55:532–549

Stockford A (2023) Assessment of vertical hydraulic connectivity in a multilayered aquifer-aquitard system in response to deep bedrock pumping using high-resolution spatiotemporal monitoring. MSc Thesis, University of Guelph, Guelph, ON, Canada

Tellam JH, Barker RD (2006) Towards prediction of saturated-zone pollutant movement in groundwaters in fractured permeable-matrix aquifers: the case of the UK Permo-Triassic sandstones. Geol Soc Spec Publ 263:1–48

Terzaghi RD (1965) Sources of error in joint surveys. Geotechnique 15(3):287–304

Underwood CA, Cooke ML, Simo JA, Muldoon MA (2003) Stratigraphic controls on vertical fracture patterns in Silurian dolomite, northeastern Wisconsin. AAPG Bull 87(1):121–142

Unonious N (2012) An evaluation of the impact of anthropogenic activities in groundwater quality in a regional bedrock aquifer: a geochemical and isotopic approach. MSc Thesis, University of Waterloo, Waterloo, ON, Canada

Wakida FT, Lerner DN (2005) Non-agricultural sources of groundwater nitrate: a review and case study. Water Res 39:3–16

Williams JH, Johnson CD (2004) Acoustic and optical borehole-wall imaging for fractured-rock aquifer studies. J Appl Geophys 55:151–159

Witthüser K, Arnepalli D, Singh DN (2006) Investigations on diffusion characteristics of granite and chalk rock mass. Geotech Geol Eng 24:325–334

Xie W, Ren B, Hursthouse AS, Wang Z, Luo X (2021) Simulation of manganese transport in groundwater using visual MODFLOW: a case study from Xiangtan manganese ore area in central China. Polish J Environ Studies 30:1409–1420